Palaeogeography, Palaeoclimatology, Palaeoecology 589 (2022) 110840

Contents lists available at ScienceDirect

Palaeogeography, Palaeoclimatology, Palaeoecology

journal homepage: www.elsevier.com/locate/palaeo

The Eocene carbonate platform of the central-western Malaguides (Internal Betic Zone, S Spain) and its meaning for the Cenozoic paleogeography of the westermost Tethys

Josep Tosquella [a], Manuel Martín-Martín [b,*], Francesco Guerrera [c], Francisco Serrano [d], Mario Tramontana [e]

[a] Departamento de Ciencias de la Tierra, University of Huelva, Huelva, Spain
[b] Departamento de Ciencias de la Tierra y Medio Ambiente, University of Alicante, Alicante, Spain
[c] Ex-Dipartimento di Scienze della Terra, della Vita e dell'Ambiente, (DiSTeVA), Università degli Studi di Urbino Carlo Bo, Urbino, Italy
[d] Departamento de Geología y Ecología, Universidad de Málaga, Málaga, Spain
[e] Dipartimento di Scienze Pure e Applicate (DiSPeA), Università degli Studi di Urbino Carlo Bo, Urbino, Italy

ARTICLE INFO

Keywords:
Carbonate platforms
Larger benthic foraminifera (LBF)
Ypresian-Lutetian
Paleoenvironmental evolution
Westernmost Tethys

ABSTRACT

The Eocene Peñicas (Almería) and Harania (Málaga) stratigraphic sections from the Malaguide Complex (Betic Cordillera, South Spain) belonging to the Mesomediterranean Microplate from the westernmost Tethys (about 35°N and 0° to 5°E according to the Eocene coordinates) have been studied. The Eocene sections cover the Cuisian to middle Lutetian deposits, which show several lithofacies representing shallow marine platform realms. Based on the fossiliferous assemblage, texture and fabrics, eight microfacies related to inner to outer ramp settings were defined. In the inner ramp of the Harania section abundant colonial corals have been recognized. The Eocene deposits are arranged into a transgressive succession composed by three minor transgressive-regressive sedimentary cycles. The Eocene fossiliferous assemblage shows a mixture of photozoan (Larger Benthic Foraminifera –LBF–, green and red calcareous algae and corals) and heterotrophic (mollusks, echinoids, bryozoans, small benthic and planktic foraminifers) elements, suggesting euphotic to mesophotic conditions in oligo-mesotrophic marine warm-waters at low-middle latitudes. This assemblage indicates a transition from photozoan to heterozoan carbonates and in particular a shift towards outer marine ramp settings. During the Early Eocene, the widespread distribution of LBF leads in the Tethyan domains to disappearance or extreme reduction of coral constructions. Nevertheless, abundant corals associated to inner ramp realms have been observed in the Harania stratigraphic section indicating that corals could continue to develop in the westernmost Tethys at the transition to the Atlantic Ocean, in contrast with respect to other Tethyan sectors. Therefore, the Ypresian-Lutetian time-span is a transitional period for the global temperature during which corals locally survived only where optimal ecologic conditions occurred, preferably in marginal contexts, as it seems to have happened in the studied area.

1. Introduction

The Paleocene-Eocene is a global mostly warm period (Kennett and Stott, 1991) called Paleocene-Eocene Thermal Maximum (PETM; Zachos et al., 2001), which maintained until the onset of a climatic cooling corresponding to the latest Eocene culminating at the Eocene-Oligocene boundary (Zachos et al., 1996). Nevertheless, successive short hyperthermal events alternating with cooler periods have been recognized (Agnini et al., 2009; and references therein). So, the onset of the late Ypresian (Cuisian, SBZ10–11) corresponds to a warm period known as early Eocene climatic optimum (EECO, 52–50 Ma; Zachos et al., 2001); later, a cool period (post-EECO cooling event; Zachos et al., 2001) dominated from the late Cuisian (SBZ12) to the early-middle Lutetian (SBZ13–14), which was interrupted by two short warmer periods, known as LLTM (late Lutetian thermal maximum) and MECO (middle Eocene climatic optimum) (Zachos et al., 2001). Others terms used in literature (Zachos et al., 2001) are Eocene Thermal Maximum −1 to −3 and Eocene Layer of Misterious Origin (ETM-1, ETM-2, ETM-3 and

* Corresponding author.
E-mail address: manuel.martin@ua.es (M. Martín-Martín).

https://doi.org/10.1016/j.palaeo.2022.110840
Received 7 October 2021; Received in revised form 25 December 2021; Accepted 6 January 2022
Available online 13 January 2022

ELMO; this last equivalent to ETM-2). In this variable context, important changes in biotic assemblages of shallow-marine environments also took place.

Many extensive Eocene carbonate platforms are recognized in different sectors of the alpine peri-Mediterranean chains and outside this area. Their distribution fall on a wide range of paleolatitude ranging from 50°N to 10°S and paleolongitude from 20°W to 80°E, according to the Eocene coordinates (Müller et al., 2019). Their shallow marine (carbonate platform) deposits are well developed into two belts along the Tethyan system (Scheibner and Speijer, 2008; Höntzsch et al., 2013; Martín-Martín et al., 2020c). A northern belt (middle latitudes: about 40°N) was located from the Pyrenees to the Tibetan region comprising the Alpine, Adriatic, Apennine, Carpathian, Great Caucasus, Hellenian, Anatolian and Indian systems), while the southern belt (mostly below 25° N) extended from Morocco to Oman, including Tunisia, Libya, Egypt and Arabia.

In these shallow marine settings, the Eocene deposits are usually represented by wide platform belts. These platforms were rich in larger benthic foraminifera (LBF) ranging from inner to open oligophotic marine conditions. It was also common the presence of interspersed seagrass and coralline algal maerl environments, and sporadic coral patch-reef constructions (Martín-Martín et al., 2001; Kazmer et al., 2003; Serra-Kiel et al., 2003a, 2003b; Vlahovic et al., 2005; Özcan et al., 2010; Rodríguez-Pintó et al., 2012; Serra-Kiel et al., 2016; Tawfik et al., 2016; Morsilli et al., 2017; Pomar et al., 2017; Hadi et al., 2019; among others). In these environments, the biostratigraphic analyses are based on benthic communities living in shallow marine waters and, especially, on LBF. Moreover, the recognized fossiliferous LBF associations have allowed accurate dating of the stratigraphic sections with a good resolution by using the Shallow Benthic Zones (SBZ) according to Serra-Kiel et al. (1998).

Previous studies show that zooxanthellate coral-reef buildups (z-corals) are widespread through shallow platforms along the central and eastern Tethys during the Eocene *p.p.* These deposits are of neither great dimensions nor dominant, because of the much widespread presence of LBF. Only recurrent coral-reef patches are scattered on the broad LBF accumulations, and developed in marine ramp settings in relation to the temperature increase (EECO, SBZ10–11; LLTM and MECO events, SBZ16–17). A general zonation and distribution of LBF and z-coral events during the Cenozoic was deduced and formally proposed by Pomar et al. (2017; and references therein).

According to Adams et al. (1990) and Langer and Hottinger (2000), the LBF distribution is restricted to a worldwide climatic belt with a minimum of temperature of 15–20 °C and controlled by the extent of low nutrient water masses. The late Ypresian (Cuisian), corresponding to the EECO event, was the peak in specific diversity in some groups as alveolinids (Whidden and Jones, 2012) and nummulitid foraminifera (Serra-Kiel et al., 1998). However, both groups suffered a significant decrease in diversity during the late Cuisian, whereas a renewed phase of increasing diversity is observed during the early Lutetian (Serra-Kiel et al., 1998; Whidden and Jones, 2012; Martín-Martín et al., 2021). So, the middle Eocene is usually considered the peak for LBF diversity in the Tethys realm, which indicate optimal conditions to make this group thrive in an intertropical belt, on broad homoclinal shallow marine ramps free to be colonized and to develop new ecological niches (Whidden and Jones, 2012; Martín-Martín et al., 2021). Under such conditions, z-corals were not very widespread however, and they were only present as small patches scattered in various ramp environments throughout the circum-Tethyan region. A relationship with eco-climate factors does not seem evident and this absence could be explained by the presence of areas with nutrient-rich deep-water upwelling (Herbig and Trappe, 1994; Scheibner and Speijer, 2008), locally controlled by terrestrial run-off. In fact, the LFB are better adapted to these conditions than corals.

A recent study (Martín-Martín et al., 2020c) concerning the upper Ypresian (Cuisian) deposits of the eastern Malaguide Units (Sierra Espuña area, SE Spain; at about 35° N and 0° to 5°E according the Eocene coordinates) pointed the presence of abundant z-coral buildups. These deposits indicate that in the westernmost Tethys (transition at mid-latitudes to the proto-Atlantic domain) coral-reefs continued to develop as opposed to similar latitudes of other southern and western Tethyan areas. In contrast, corals were found neither in the pene-contemporaneous low latitude sedimentary successions of the moroccan Ghomaride Unit and the north-african Rif (Maaté et al., 2000; Hlila et al., 2007) nor in the Atlas platform (Morocco and Tunisia: Herbig and Trappe, 1994; Scheibner and Speijer, 2008). In these north African areas benthic associations are characterized by oyster reefs, coralline algae and some heterotrophic elements as bryozoans, so noteworthing the absence of LBF and corals with respect to coeval platforms of the northern margin of the Mediterranean Tethys.

The paleogeography of the westernmost Tethys reconstructed by many authors (e.g., Guerrera et al., 2021), showing the transition from a narrow and deep ocean realm as the Maghrebian Flysch Basin (MFB) to the Atlantic Ocean can explain fauna variations in these domains (Martín-Martín et al., 2020a, 2020b, 2020c).

The present study proposes a lithostratigraphic reconstruction and correlation of the Eocene successions outcropping in the Almeria and Malaga sectors, and the description and interpretation of the micro- and macrobiofacies recognized in these shallow-water marine successions belonging to the central-western Malaguides (Internal Betic Zone: *IBZ*) which was part of the Jurassic-lower Paleogene passive margins of the Mesomediterranean Microplate (Guerrera et al., 2021).

The study reconstructs the main evolutionary stages and related paleoenvironmental features of two Eocene *p.p.* carbonate platforms of the Betic Cordillera located in the Almería and Málaga provinces (S Spain) in the westermost Tethys. The results are discussed and compared with coeval successions of other sectors of the Tethyan Domain.

2. Materials and methods

The methodological approach consists of field geological observations, including tectonic controls, reconstruction of the Eocene stratigraphic record, lithological features, sedimentological observations, and laboratory analyses, mainly addressed to define the fossiliferous content especially for the large foraminifera, which are very abundant at different stratigraphic levels.

The analyzed successions belong to the Malaguide Complex (Betic Cordillera) and the study areas are located in two sectors (Fig. 1): (i) Velez Rubio in the Almería province (Central Malaguides) and (ii) El Palo in the Malaga province (Western Malaguides). In particular, two Eocene successions have been analyzed and sampled in detail, corresponding to the Peñicas section in Vélez Rubio, Almería (log 1; thickness 115 m), and El Palo section in the Harania area, Málaga (Log 2; thickness 55 m), which show some well correlated stratigraphic intervals. During the fieldwork several different litho-biofacies were differentiated and described (Table 1). Nineteen samples from log 1 and 6 samples from log 2 were collected for thin sections (2,0 × 3.0 cm), which were prepared for microfacies analysis (Table 2, Fig. 5) by using an optical microscope Nikon Eclipse E 200, in order to interpret paleoecological features and depositional paleoenvironments. Photographs were obtained by a digital camera (Nikon DS-Fi2) and images were transferred to a PC computer using a Nikon's Digital Sight DS-U3 microscope camera controller and treated with the microscope imaging software Nikon NIS Elements F4.

The microfacies analysis and lithology description followed the methodology of Flügel (2010) and the terminology of Embry and Klovan (1971). In order to differentiate microfacies assemblages, all the allochem components and matrix were characterized and visually estimated in thin sections (Table 2).

The identification of nummulitid foraminifera followed Loeblich and Tappan (1987). *Assilina* genus includes both traditional evolute tests with low spiral growth forms (*Assilina* s.s.) and the evolute open spiral growth forms with simple septa (not folded) named 'operculiniform

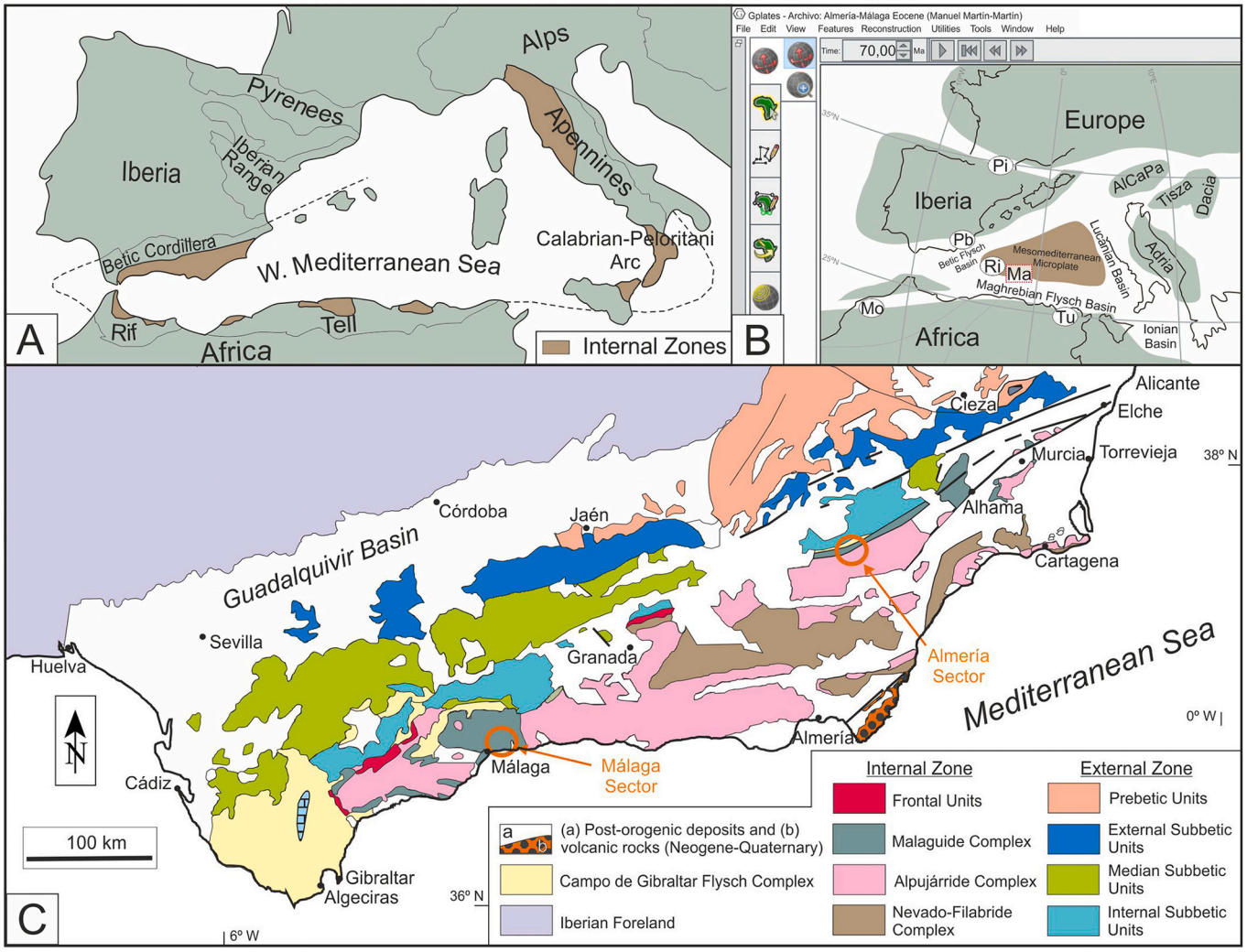

Fig. 1. Introduction to the geological framework. A) Western Mediterranean alpine chains: Betic-Rif Cordillera, Tell, Apennines; B) Mesozoic Paleogeographic sketch of the central-western Mediterranean area modeled by GPlates software according to Guerrera and Martín-Martín (2014; modified), with location of the studied and compared sectors: Ma (Malaguides of the Internal Betic Zone, including the areas studied in this paper); Pi (Pyrenees), Pb (Prebetics of the External Betic Zone), Ri (Ghomarides and Dorsal of the Internal Rifian Zone), Mo (Moroccan External Zone), Tu (Tunisian Tell); C) Synthetic geological map of the Betic Cordillera with location of the studied areas.

Assilina' according to Tosquella and Serra-Kiel (1998).

3. Geological setting

The Betic Cordillera constitutes the westernmost branch of the Alpine peri-Mediterranean chains (Fig. 1A) derived from the Alpine evolution of the western Tethyan area (Fig. 1B). This cordillera (Fig. 1C) is classically divided into the Internal and External Zones, separated by the Flysch Complex by means of interposed units (Martín-Algarra, 1987). In turn, the Internal Betic Zones (IBZ) are made up of three stacked nappe complexes (Fig. 1C): Nevado-Filábride, Alpujárride and Maláguide (Martín-Algarra, 1987) complexes, plus the so-called Frontal Units (Serrano, 1997; Serrano and Guerra-Merchán, 2004; Martín-Algarra et al., 2004; Jabaloy-Sánchez et al., 2019). The Mesozoic-Cenozoic lithostratigraphy of the Maláguide Complex reflects the tectono-sedimentary evolution occurred in the southwestern part of the so-called Mesomediterranean Microplate (*MM*) located between Iberia-Eurasia and Africa Plates and surrounded by some Tethyan oceanic branches (Fig. 1B) (Guerrera et al., 2005; Guerrera and Martín-Martín, 2014; Guerrera et al., 2021; Martín-Martín et al., 2006, 2020a, 2020b, 2020c; and references therein).

The Malaguide Complex (Fig. 1C) shows a Paleozoic basement mainly made up of slates and graywackes, with subordinated limestones and siliceous levels, unconformably followed by Triassic continental redbeds and Jurassic carbonate platform deposits, which are covered by a thin Cretaceous marine pelagic succession topped by shallow to deep marine Cenozoic rocks (Jabaloy-Sánchez et al., 2019). The deposition of the youngest Cenozoic beds was coeval to the main deformation of the Betic Internal Zone thrust stack, from which the Malaguide Complex constituted its wedge-top (Martín-Martín et al., 1997a, 1997b, 1998; Perri et al., 2017; Martín-Martín et al., 2020c; and references therein). Regarding the Eocene Malaguide succession, it consists of shallow marine carbonate deposits made of alveolina and nummulite-rich limestones, and coral-rich levels in some cases (Xiquena and Jardin fms of Geel, 1973; Espuña, Malvariche and Canovas Fms of Martín-Martín, 1996; see also Serrano et al., 1995, and Martín-Martín et al., 2020c, 2021) and lagoonal to mangrove deposits with locally rich Nypa-bearing pollen associations (Kevdes et al., 1996; Solé de Porta et al., 2007), marls bearing lignite beds and limestones with gastropods and bivalves (Valdelaparra Fm of Martín-Martín, 1996).

The Cenozoic of the Malaguide Complex has been studied in two sectors (Fig. 2): Almería (Fig. 3A) and Málaga (Fig. 3B), both located in South Spain, in central and western Malaguides respectively. The studied successions comprise two informally defined stratigraphic Cenozoic

Table 1
Lithostratigraphy of the Peñicas and Harania stratigraphic sections (Malaguide Complex, Internal Betic Zone) in the Vélez Rubio (Almería, log 1) and El Palo (Málaga, log 2) localities, and the short description of lithofacies and fossils recognized in the field.

Peñicas stratigraphic section (log 1) – Locality: Vélez Rubio (Almería)

Thickness (m)	Formation (thickness) *Sª Espuña equivalents*	Samples	Age	Lithofacies	Fossils recognized in the field	Micro-facies
6		CH 20, 13	middle Lutetian *p.p.* (SBZ 14)	***Lithofacies F1,*** Poorly stratified algal limestones and fine to medium grained thick-bedded biocalcarenites with amalgamation surfaces.	Abundant flat large nummulites, algae (rhodoliths), sometimes up to some cm in size.	*Mf6*
12		CH 19		***Lithofacies N,*** Pinkish homogeneous silt-sandy pelites	Abundant large nummulites Planktonic foraminifera visible with a hand lens	*Mf5*
5		12, CH 17		***Lithofacies M,*** Biocalcarenites and alternating limestones and sandy-pelites, and sometimes brecciated limestone beds	Flat large nummulites	*Mf3*
8		CH 16		***Lithofacies N,*** Pinkish homogeneous silty-sandy pelites	Large nummulites Planktonic foraminifera visible with a hand lens	*Mf5*
20		10, 11	early Lutetian *p.p.* (SBZ 13)	***Lithofacies M,*** Biocalcarenites and alternating limestones and sandy-pelites, and sometimes brecciated limestone beds	Abundant flat large nummulites	*Mf3*
24	**XIQUENA FM (115 m)** ***Espuña-Malvariche*fms**	9		***Lithofacies R,*** Coarse and cemented biocalcarenites (fine to medium grained and with much large fossils); presence of brecciated structures	Abundant large nummulites	
5		7, 8		***Lithofacies G,*** dark brownish thick-bedded micritic limestones with amalgamation surfaces and with miliolids	Abundant miliolids, occasional alveolinids and orbitolites (lagoon)	
8		6	Cuisian *p.p* . (SBZ 10–12)	***Lithofacies F,*** Thick-bedded calcarenites with amalgamation surfaces and stratified decimetric limestones (fine to medium grain size) with up to 0,3 cm in size rounded quartz grains	Abundant alveolinids, less frequent nummulites often in pockets and bands, very rich in coarser fossils and with scarce matrix	*Mf2*
17		CH 14, 5 2, 3, 4		***Lithofacies A,*** Thick-bedded calcarenites with amalgamation surfaces and white massive alveolina limestones	Very frequent large alveolinids up to 1–2 cm in size; scarce nummulites	*Mf2, Mf4 and Mf7*
10		CH13, 1		***Lithofacies D,*** Sandy calcarenites, poorly stratified bio-calcarenites with quartz pebbles, occasionally with plane parallel lamination; the base of the beds is often conglomeratic (with limestone clasts up to 4–8 cm)	Very abundant nummulites, alveolinids and echinoderms (without algae) often concentrated in pockets or in coarser levels (fine to coarse sand grain size)	*Mf1*
Unconformity (erosive surface)						
>30?	**CASTILLÓN FM**	–	Jurassic	Massive limestones		

Harania stratigraphic section (log 2) – Locality: El Palo (Málaga)

Thickness (m)	Formation	Samples	Age	Lithofacies	Fossils recognized in the field	Micro-facies
5		Ma 18 Ma 17	early Lutetian *p. p*. (SBZ 13)	***Lithofacies* F2**, Algal limestones and poorly stratified thick-bedded fine to medium grained biocalcarenites with amalgamation surfaces.	Abundant alveolinids, corals and algae; less frequent nummulites	*Mf8*
8		–		***Lithofacies B,*** White to grey marly pelites and clays with lignite beds		*Mf7*
17		Ma 16		***Lithofacies A,*** Massive white alveolina limestones	Very frequent up to 1–2 cm large alveolinids; nummulites are missing	*Mf2*
5	**HARANIAFM (55 m)** ***Espuña-Valdelaparrafms***	–		***Lithofacies B,*** White to grey marly pelites and clays with lignite beds		*Mf7*
6		Ma 14	Cuisian *p.p.* (SBZ 10–12).	***Lithofacies G,*** Thick-bedded blackish-gray and brownish micritic limestones with amalgamation surfaces and with miliolids	Abundant miliolids	*Mf4*
10		Ma 13		***Lithofacies A,*** Massive white alveolina limestones		*Mf2*
4		Ma 12		***Lithofacies D,*** Sandy calcarenites, poorly stratified bio-calcarenites with rounded quartz pebbles, occasionally plane parallel lamination; the base of the beds is often conglomeratic (limestone clasts up to 4–8 cm).	Very abundant nummulites, alveolinids and echinoderms (without algae) often concentrated in pockets or in coarser levels (fine to coarse grain size)	*Mf1*
Tectonic contact						
>10?	**PALEOCENE FM** ***Mula Fm***	–	Paleocene	Microcodites, conglomerates and calcarenites with Microcodium	Abundant Microcodium	

Table 2
Microfacies with their description and relative abundance of components, and depositional environment interpretation. Studied samples and fossil content (commom, abundant, present and/or rare) are also shown.

Microfacies	Samples	Description	Fossils and not skeletal grains common and/or abundant*	Fossils and not skeletal grains present and/or rare	Depositional environment
Mf1	VR 1 CH 13 MA 12	Quartzarenite with LBF	*Nummulites**, rounded quartz grains*, *Alveolina, Assilina, Discocyclina,* rhodoliths, rotaliids, discorbids, textularids; *Glomalveolina*, *Amphistegina,* mollusks; annelids *(Ditrupa);* echinoid debris	Miliolids, *Orbitolites,* operculiniform *Assilina;* dasyclades, udotacean *Ovulites*; ostracods; bryozoans	'Transgressive reworked deposit' in inner to mid ramp transition Mesophotic environment
Mf2	VR 2 VR 3 VR 4 VR 5 **CH 17** MA 13 MA 16 CH 14	Porcelaneous LBF packstone-grainstone	*Alveolina**, *Glomalveolina**, *Orbitolites**, miliolids*, discorbids*, dasycladal algae*, *Nummulites,* rotaliids, amphisteginids, textularids; geniculate coralline algae; mollusks (gastropods, ostreids and other pelecypods); echinoid debris; peloids; cortoids: reworked and rounded grains of alveolinids, miliolids and rotaliids	Operculiniform *Assilina, Discocyclina*, planktic foraminifers; crustose coralline remains; ostracods; annelids (*Ditrupa*)	Inner ramp seagrass Euphotic subtidal environment
Mf3	VR 6 VR 7 VR 9 VR 10 VR 11 VR 12	Hyaline LBF packstone	*Nummulites**, *Assilina**, *Amphistegina**, rotaliids (*Gyroidinella, Rotalia*)*, echinoid debris*, hyaline encrusting foraminifers, operculiniform *Assilina, Discocyclina, Fabiania,* discorbids, textularids; crustose and geniculate coralline algae; annelids (*Dytrupa*); quartz grains	*Sphaerogypsina,* miliolids, planktic foraminifers; bryozoans; ostracods; mollusk remains	Middle ramp nummulitid accumulations Mesophotic environment
Mf4	VR 8 MA 14	Miliolid and peloidal grainstone	Miliolids*, peloids*, discorbids, rotaliids, dasyclade algae; ostracods; mollusks (gastropods, pelecypods); quartz grains*	*Orbitolites,* textularids; geniculate coralline algae; echinoid debris	Protected inner ramp lagoon Euphotic upper subtidal environment
Mf5	CH 16 CH 19	Quartzsiltitic wackestone with bolivinids and planktic foraminifers	Bolivinids, planktic foraminifers; ostracods; mollusk remains; quartz grains* and sparse glauconite grains	Unspecific rotaliids; echinoid remains	Outer ramp Oligophotic environment
Mf6	CH 20 VR 13	*Nummulites*-foralgal packstone	Crustose coralline algae* (*Lithothamnion?, Sporolithon, Lithoporella*); hyaline encrusting foraminifers (*Solenomeris, Acervulina, Planorbulina*)*, *Nummulites**, *Amphistegina**, *Orbitolites,* haddonids, *Assilina, Discocyclina, Fabiania, Sphaerogypsina,* rotaliids, discorbids, miliolids; geniculate coralline algae; annelids; echinoid debris	Operculiniform *Assilina,* textularids, planktic foraminifers; bryozoans; mollusk remains	Proximal middle ramp maërl and macroid beds on nummulite accumulations Mesophotic environment
Mf7		Marly wackestone with miliolids and ostracods	Miliolids; ostracods; plant debris; oogonia and thallus remains of charophytes	cm-thick silt and lignite beds	Restricted inner ramp lagoon Euphotic upper subtidal environment
Mf8	MA 17 MA 18	Coral-foralgal boundstone	Colonial corals*; hyaline encrusting foraminifers* (acervulinids, planorbulinids, homotrematids); miliolids*, crustose coralline algae* (*Lithoporella, Lithothamnion?*); *Alveolina, Orbitolites,* rotaliids, discorbids, *Fabiania cassis*; textularids, haddonids, udotacean (*Ovulites*) and dasyclade green algae; ostracods; annelids; mollusks (gastropods, pelecypods); echinoid debris	Discorbids, planktic foraminifers; geniculate coralline algae; bryozoans; boring bivalves	Coral-algal inner ramp Euphotic subtidal environment

formations: the Xiquena fm (Peñicas stratigraphic section) in the Vélez Rubio area, near Almería (Geel, 1973) and the Harania fm (El Palo stratigraphic section) in the Harania sector, near Malaga (Serrano et al., 1995). Both stratigraphic formations have formal equivalents in the Sierra Espuña area (Murcia province) (Table 1): Espuña, Valdelaparra and Malvariche fms (Martín-Martín, 1996; Martín-Martín et al., 2020c, 2021). Both formations have been strongly deformed during the main orogenic events, which mainly occurred during the Oligocene and the Early Miocene. These formations were previously studied by a petrographical, mineralogical and geochemical point of view, in order to characterize the clastic supply (Critelli et al., 2020).

4. Studied outcrops

4.1. Structural framework of the studied outcrops

The Peñicas section (Figs. 2A, 3A, C–D and 3G–H) is located a few hundred of metres south of Vélez-Rubio and shows good outcrop conditions (Geel, 1973; Voermans et al., 1978). The Eocene succession unconformably rests over the Jurassic succession by mean of an unconformity. The Eocene oucrop is made of a normal succession (although locally can be overturned in near areas) made of alternations of calcareous and marly-sandy beds where it has been measured and sampled (Figs. 2A and 3A). The oldest Cenozoic deposits in the Harania Cement Factory, near El Palo (Fig. 2B) are Paleocene-Eocene sandy--calcareous and conglomeratic deposits rich in Microcodium debris and crusts (Serrano et al., 1995). In this area, noticeable S and E vergent thrusts locally stack Paleozoic deposits onto its (originally stratigraphically overlying) Triassic and Meso-Cenozoic cover (both also affected by thrusts and folds with overturned limbs), and a transgressive Burdigalian *p.p.* succession affected by late normal faults seals some of the mentioned structures in a few small outcrops in the Harania Cement Factory area (Fig. 3B) and in other nearby areas around Malaga city (Serrano et al., 1995). Even if the Paleogene succession is strongly deformed and partially covered, it was possible to study and sample a overturned stratigraphic Eocene interval (Fig. 3B and F).

4.2. Lithostratigraphy and chronostratigraphy

Ten lithofacies (Table 1) were recognized in the studied successions

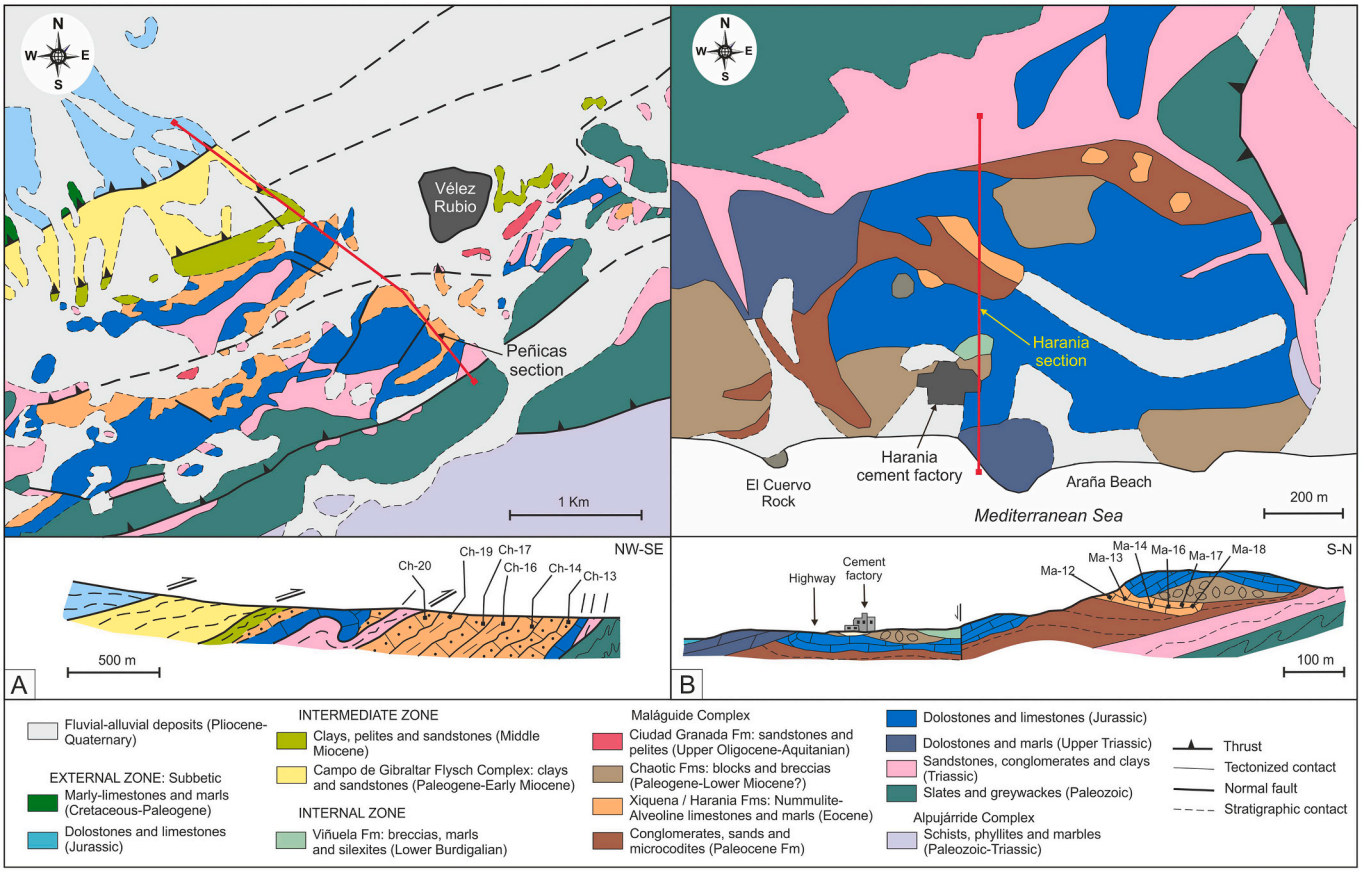

Fig. 2. Detailed geological maps and cross-sections of the study sectors: A) Vélez Rubio (Almería area) with location of the Peñicas stratigraphic section; B) El Palo (Málaga area) with location of the Harania stratigraphic section.

(A, B, D, F, F1, F2, G, M, N and R) and the nomenclature used follows as much as possible the letters defined by Martín-Martín et al. (2020c and 2021).

The succession measured in the Vélez Rubio Corridor area (log 1) includes a Jurassic substratum of massive limestones (> 35 m thick) on which the Eocene *p.p.* Xiquena outcrop from Geel (1973) (115 m thick) rests by means of an evident and significant regional unconformity. An early-middle Cuisian (SBZ10–11) age is dated in the base of the section (VR 6 sample) by the presence of *Nummulites burdigalensis burdigalensis* and *N.* cf. *planulatus*. Samples collected in the middle part of the section (VR 9–10), with *Fabiania cassis* and *Nummulites* aff. *obesus,* respectively, indicate an early Lutetian (SBZ13) age. Finally, samples from the upper portion of the section (VR 12–13), with *Nummulites* aff. *millecaput,* indicate a middle Lutetian age (SBZ 14; Fig. 4). In the studied outcrop different lithofacies (from bottom to top: D, A, F, G, R, M, N and F1) have been recognized (photos A, C, D, G and H in Fig. 3), which are synthetically described in Table 1, and represented in Fig. 5. The succession shows a variety of lithotypes such as: sandy calcarenites, thick-bedded calcarenites with amalgamation surfaces, sandy pelites, micritic limestones, biocalcarenites, which are variously associated to form different lithofacies associations. These rocks often show a fossiliferous content that allow characterizing each lithofacies. The most significant fossiliferous assemblage including alveolines, miliolids, nummulites and large nummulites and algae has also been used for paleoenvironmental interpretations (see below).

The Harania succession reconstructed in the El Palo sector (log 2) comprises a Paleocene substratum constituted by microcodites and conglomerates (> 45 m thick), onto which the Eocene *p.p.* of the Harania succession (55 m thick) rests by mean of a well marked regional unconformity. The presence of a nummulitid assemblage with the *Nummulites subramondi* (recognized in thin sections; Ma-13 sample) dated the base of the section as early-middle Cuisian (SBZ10–11). Instead, the presence of *Nummulites* cf. *praelorioli* and *Fabiania cassis* (sample Ma-17) indicates a early Lutetian age for the top (SBZ 13; Fig. 4). In this outcrop, which has been measured and sampled within the quarry close to the cement factory (Figs. 2B and 3B), different lithofacies (from below: D, A, G, B, and F2) have been recognized (photos B and F in Fig. 3), which are synthetically described in Table 1 and represented in Fig. 5. The Harania succession shows also a variety of lithotypes similar to those previously mentioned for the Peñicas outcrop. In particular, locally thick-bedded sandy calcarenites with amalgamation surfaces, marly pelites with lignite beds occur, showing variable fossiliferous content that characterizes most of the defined lithofacies and microfacies. The most significant fossiliferous assemblages (alveolines, miliolids, nummulites, corals and algae) and microfacies types been used for paleoenvironmental reconstructions, as shown later.

5. Microfacies description

Based on the fossiliferous assemblage, texture and fabric, eight microfacies (***Mf1*** to ***Mf8***) were recognized and numbered according to the first appearance in the succession (Table 2; Figs. 5, 6 and 7). The identified microfacies distribution is as follows: ***Mf1*** to ***Mf6*** in the Peñicas section (log 1); and ***Mf1***, ***Mf2, Mf4, Mf7*** and –***Mf8*** in the Harania section (log 2), as summarized in Table 2 and described below.

5.1. Mf1 – Quartz-rich calcarenites withLBFpackstone (Table 2; Figs. 5, 6 and 7)

This poorly- to moderately-sorted microfacies is made up of

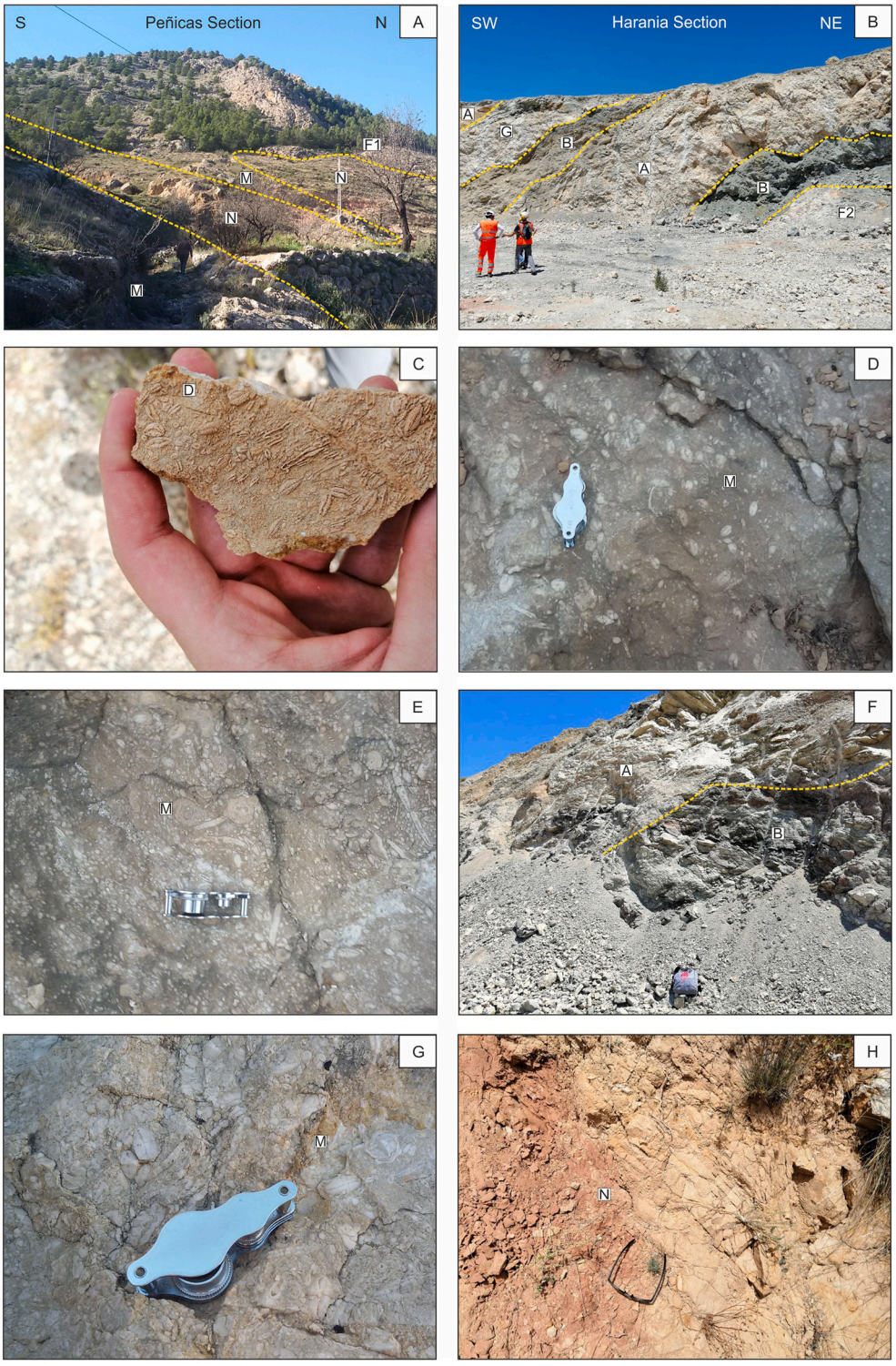

Fig. 3. Field photographs of the main lithofacies. A) Peñicas Section with location of lithofacies; B) Harania Section with location of lithofacies; C) Detail of nummulite-rich limestone in the lower part of Peñicas section (Lithofacies D); D) Detail of nummulites in the middle part of the Peñicas section (Lithofacies M); E) Detail of a limestone bed rich in flat nummulite in the upper part of the Peñicas section (Lithofacies M); F) Black beds (lagoonal-marshy) in the upper part of the Harania section (Lithofacies B); G) Detail of a limestone bed rich in rounded nummulites in the upper part of the Peñicas section (Lithofacies M); H) Pinkish marly beds with sands (open platform) in the upper part of the Peñicas section (Lithofacies N).

abundant rounded fine to medium quartz and feldspar (20–25%) grains with a well diversified biotic assemblage, which is dominated by LBF (Fig. 7, photo 1). As regards the bioclastic component, the main elements recognized are represented by *Nummulites* (15%), *Assilina* (5%), *Alveolina* (10%), *Discocyclina* (5–10%), rotaliids (5%), discorbids (5%) and textularids (5%) in an echinoid debris-rich matrix (5–10%), where syntaxial cement is frequent. Other common components are: *Glomalveolina* (2–3%), *Amphistegina* (2–3%), miliolids (2–3%), annelids (*Dytrupa*) (2–3%), crustose coralline (2–3%) and mollusk remains (2–3%) and occasionally dasycladales, udotacean *Ovulites*, ostracods, bryozoans, *Orbitolites* and operculiniform *Assilina* remains. This microfacies is present at the base of both studied stratigraphic sections with a thickness of 5 m in the Harania section and of 10 m in the Peñicas section, and corresponds to the lithofacies D (sandy calcarenites with quartz pebbles; Table 1).

5.2. *Mf2 - Porcelaneous LBF packstone-grainstone (Table 2; Figs. 5, 6 and 7)*

This moderately- to well-sorted microfacies shows a fossil association

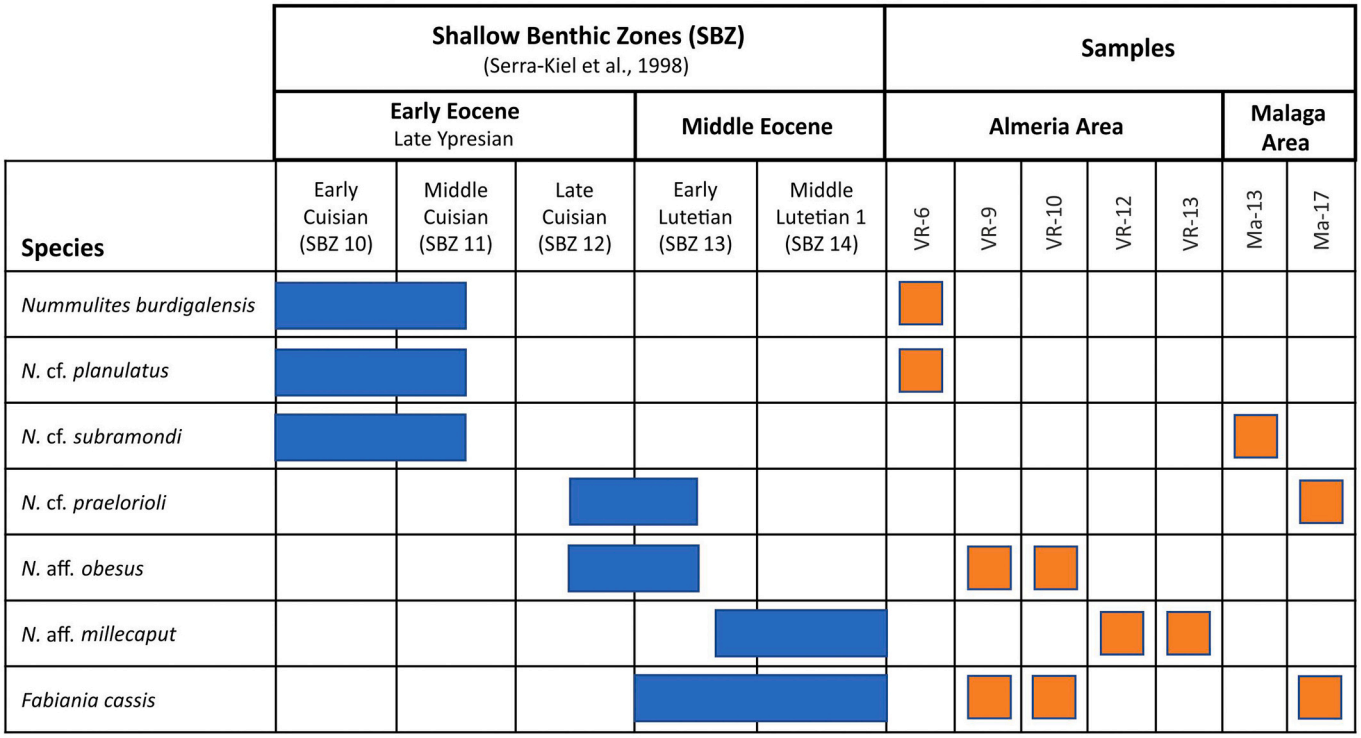

Fig. 4. Biochronostratigraphic distribution of LBF recognized in the Lower-Middle Eocene deposits of the central and western Malaguides. Stratigraphic range of the species based on data from Serra-Kiel et al. (1998) and Tosquella and Serra-Kiel (1998).

(Fig. 7, photo 2) mainly constituted by alveolinids (*Alveolina* and *Glomalveolina*), (15–20%), miliolids (10%) and rotaliid (5%) tests, even if many of them are represented by reworked rounded grains. Other abundant components are variously shaped micritic grains (10–15%), mollusks (10%), dasycladacean algae (5–10%), discorbids (5–10%), textularids (5–10%), *Orbitolites* (5%), *Nummulites* (5%), *Amphistegina* (2–3%) and echinoid debris (5%). Tests of operculiniform *Assilina, Discocyclina,* planktic foraminifers, geniculate coralline algae, ostracods and annelids (*Ditrupa*) have been observed, occasionally within an undefined recrystallized matrix. This microfacies is present in the lower part of the Peñicas section for a thickness of 17.5 m, and in a wide near to 30 m thick portion of the Harania section, corresponding to the lithofacies A *p.p.* (thick-bedded calcarenites with amalgamation surfaces with alveolines; Table 1, Fig. 5).

5.3. *Mf3 - Hyaline LBF packstone (Table 2; Figs. 5, 6 and 7)*

This microfacies is poorly-to moderately-sorted, and is constituted by abundant tests (Fig. 7, photo 3) of *Nummulites* (25–30%), *Assilina* (15–20%), *Discocyclina* (10–15%), echinoid debris (5–10%) and, locally, abundant rounded fine-sized quartz grains (5–10%). Other common components are: rotaliids (5%), miliolids (5%), *Alveolina* (2–3%), *Amphistegina* (2–3%), textularids (2–3%), udotacean *Ovulites* (2–3%), annelids *Ditrupa* (2–3%) and bryozoan remains (2–3%). Tests of *Orbitolites, Glomalveolina, Sphaerogypsina,* ostracods, and remains of crustose coralline, dasycladales and mollusks appear only occasionally in the matrix. This microfacies is only checked for a total thickness close to 100 m in the Peñicas section and corresponds to the lithofacies A *p.p.* (thick-bedded calcarenites with amalgamation surfaces with alveolines), lithofacies F (thick-bedded calcarenites with amalgamation surfaces with nummulites), lithofacies R (coarse calcarenites with large nummulites) and lithofacies M *p.p.* (biocalcarenites with flat large nummulites) (Table 1, Fig. 5).

5.4. *Mf4 – Miliolid and peloidal grainstone (Table 2; Figs. 5, 6 and 7)*

Moderately- to well-sorted microfacies constituted mainly by miliolids (20–25%) and variously shaped micritic peloids (15–30%) of uncertain origin (Fig. 7, photo 4). Discorbids (5–10%), ostracods (5–10%), echinoid debris (5–10%), mollusks (5%), rotaliids (2–3%) and textularids (2–3%) represent also an important component. Fine-sized subangular quartz grains have a variable amount, near 30% in the Harania section and 5–10% in the Peñicas section. Other bioclastic components are spirolinids, unspecific hyaline encrusters, agglutinate and hyaline small benthic foraminifers, and geniculate coralline algal remains. This microfacies is present in the lower part of the Peñicas section for a thickness of 3,5 m, and in the lower portion of the Harania section with a thickness near to 5 m, and corresponds to the lithofacies G (micritic limestones with miliolids; Table 1, Fig. 5).

5.5. *Mf5 - Quartzsiltitic wackestone with bolivinids and planktic foraminifers (Table 2; Figs. 5, 6 and 7)*

This moderately-sorted (Fig. 7, photo 5) microfacies,which shows a scarce bioclastic content, is mainly constituted by hyaline small benthic foraminifers (bolivinids) (10%), planktic foraminifers (5–10%) and subangular fine-sized quartz grains (5–10%). Other common components are unspecific rotaliids (2–3%), fine-walled ostracods (2–5%), small mollusk remains (2–5%) and dispersed glauconite grains (2–3%). Echinoid debris can be occasionally present. This microfacies has been recognized in the upper part of the Peñicas section to characterize two intervals for a total thickness of about 26 m, and it corresponds to the hardest and most calcareous beds intercalated in the lithofacies N (pinkish sandy pelites and marls; Table 1, Fig. 5).

5.6. *Mf6 – Nummulites-foralgal packstone (Table 2; Figs. 5, 6 and 7)*

This microfacies, which is poorly- to moderately-sorted, shows a bindstone to packstone texture (Fig. 7, photo 6) with abundant crustose

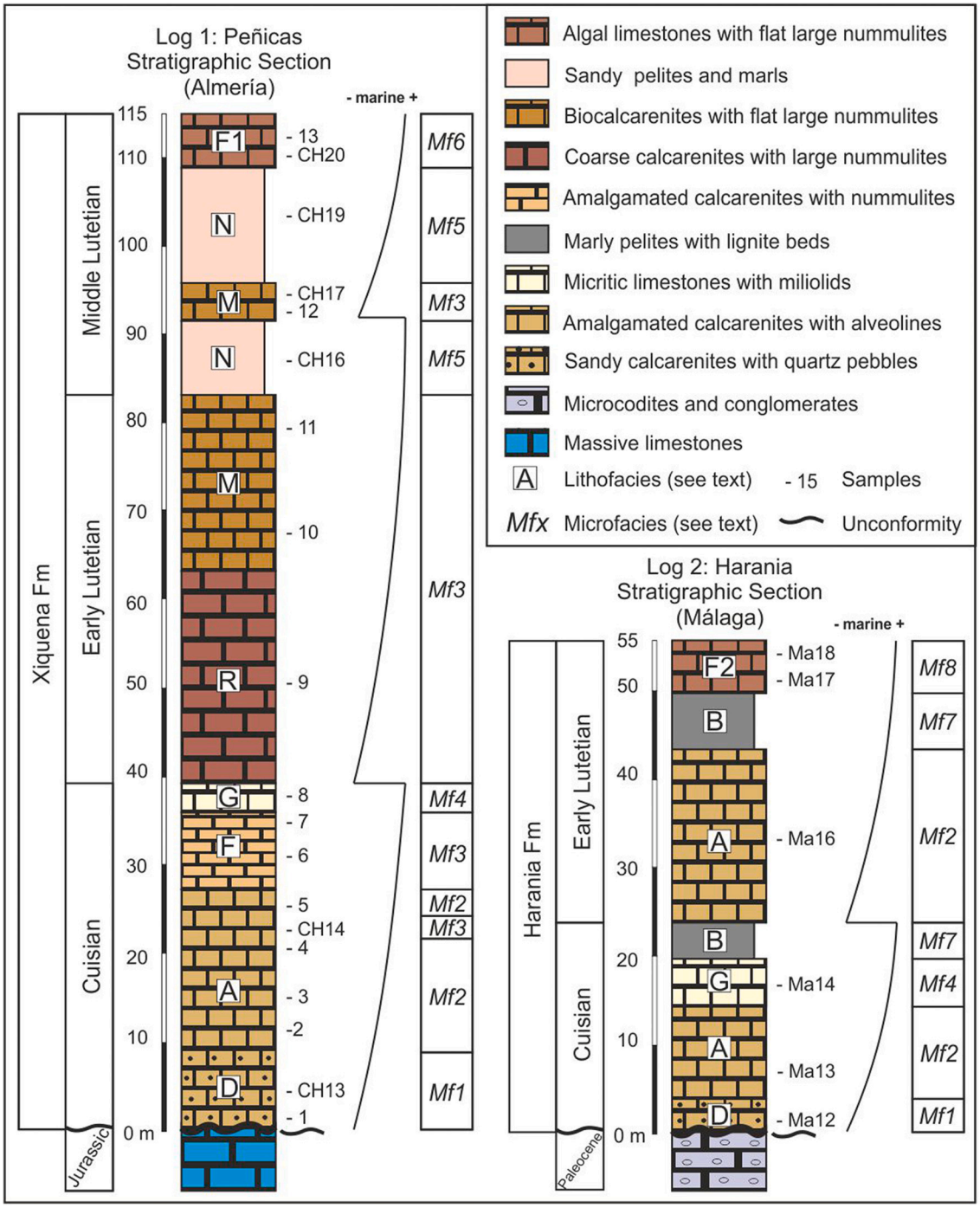

Fig. 5. Stratigraphic sections with the vertical distribution of the defined lithofacies (Table 1) and microfacies (Table 2). Sea level trends and location of the analyzed samples are also shown.

coralline algae (*Lithothamnion?, Sporolithon* and *Lithoporella*) in small to medium-sized free warty to lumpy rhodoliths and coralline fruticose branches (ϕ: 2–10 mm) (10–15%) wrapped by hyaline encrusting foraminifers (10–15%). Tests of *Nummulites* (20–25%), *Assilina* (5–10%), *Amphistegina* (5–10%), rotaliids (10–15%), and echinoid debris (10–15%) are abundant. Sometimes *Nummulites* tests make up the core of multilayered red algae encrusting successions with flattened thalli devoid of protuberances ('encrusting' *sensu* Woelkerling et al., 1993) on nummulite tests (Type 2 of Nebelsick and Bassi, 2000), with layers of hyaline encrusting foraminifers (*Solenomeris ogormani, Acervulina linearis, Planorbulina* aff. *uva* and *P.* sp). Common components distributed in the carbonate matrix are represented by the cymbaloporid *Fabiania cassis* (2–3%), annelid worm tubes (5%), coral fragments (2–3%), discorbids (3–5%), miliolids (2–3%), bryozoans (5%), echinoid debris (2–3%), and ostreid remains (2–3%). Other components such as *Discocyclina, Sphaerogypsina, Orbitolites,* planktic foraminifers, and dasycladacean algae have been observed occasionally. This microfacies is only present in the uppermost part of the Peñicas section for a thickness of 0,6 m, and is included in the lithofacies F1 (algal limestones with flat large nummulites; Table 1, Fig. 5).

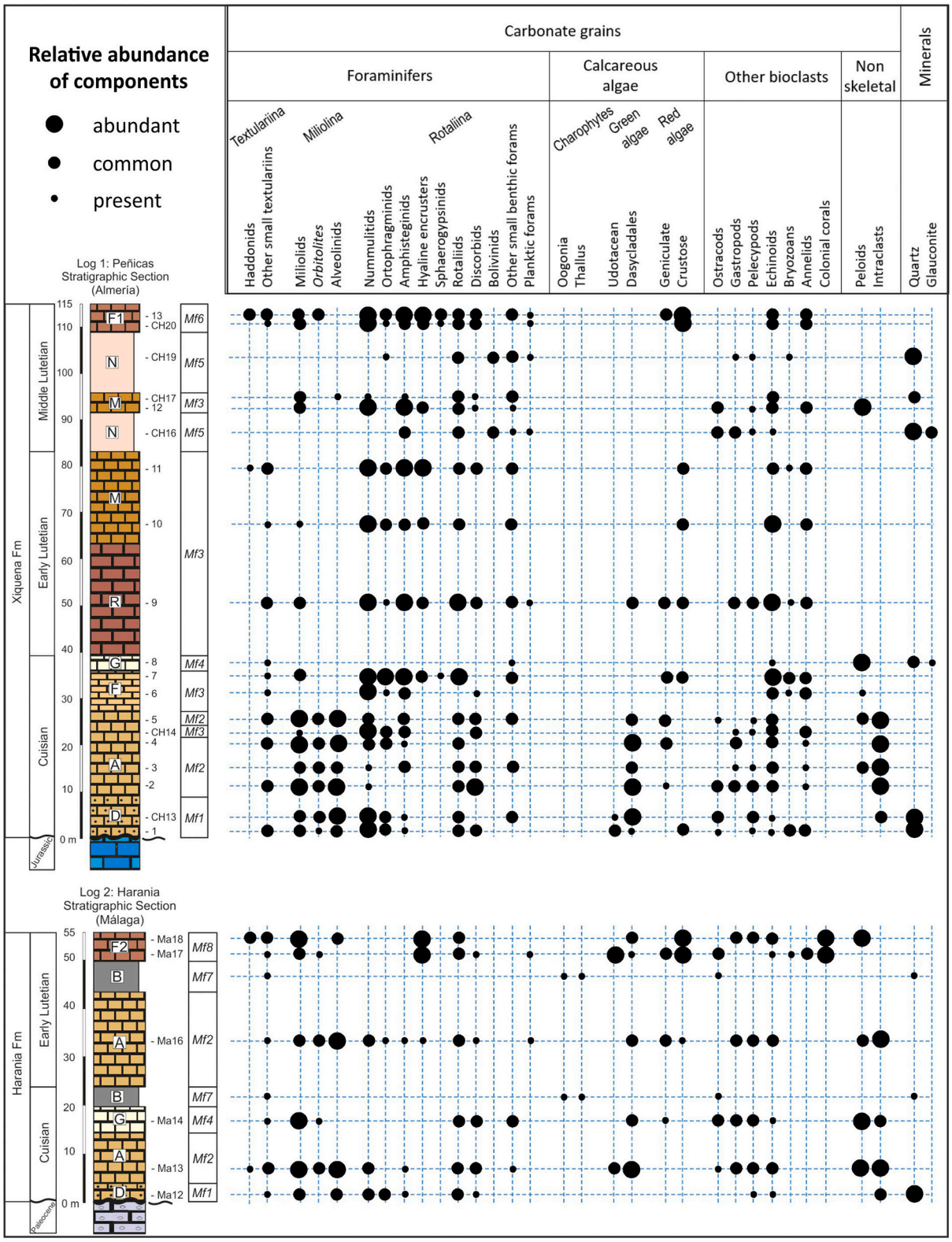

Fig. 6. Relative abundance of components recognized in the studied thin sections of samples from the Peñicas and the Harania sections (Table 2).

5.7. *Mf7 – Marly wackestone with miliolids and ostracods (Table 2; Figs. 3F, 5 and 6)*

This lithofacies is constituted by a blackish marly wackestone with interspersed thin beds (cm-thick) of silts and lignite fragments. Fossil plant debris, scattered miliolids, thin-walled ostracods, and some oogonia of charophytes constitute the poor biotic content, which has been recognized only in the field because it was not technically possible to prepare thin sections of these levels. This microfacies is only present in the Harania section to mark two separate intervals located in the middle and upper part of the section, with a thickness of 4.0 m and 6.5 m respectively, and is included in the lithofacies B (marly pelites with

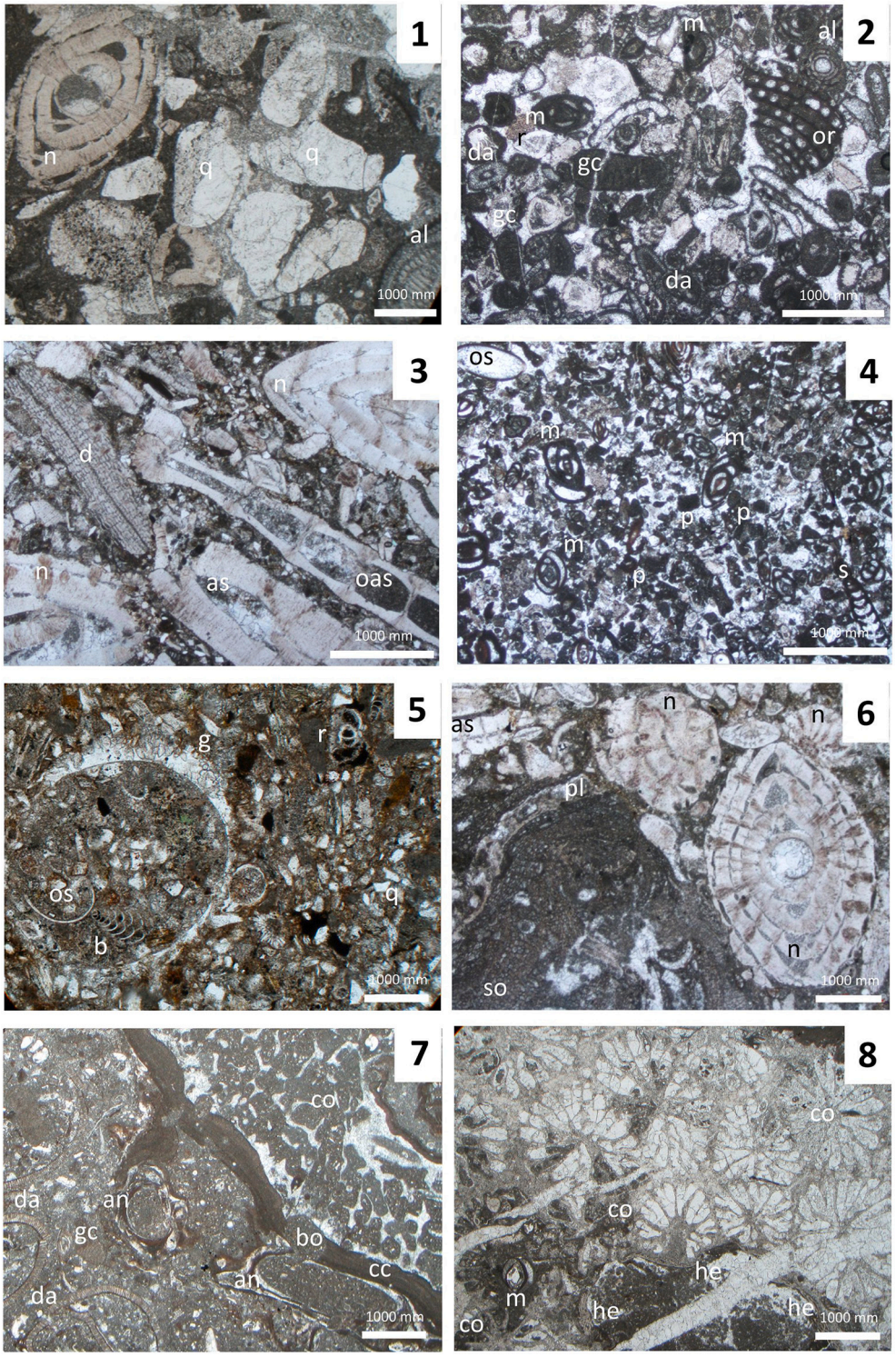

Fig. 7. Microfacies from the Peñicas and Harania sections: 1) Mf-1, sample CH-13; 2) Mf-2, sample Ma 16; 3) Mf-3, sample VR-6; 4) Mf-4, sample VR-8; 5) Mf-4, sample Ma-14; 6) Mf-5, sample CH-16; 7) Mf-6, sample VR-13; 8) Mf-7, sample Ma-18. Scale bar: 1000 mm. Key: al, alveoline; an, annelid; as, assiline; b, bolivinid; bo, boring; cc, crustose coralline algae; co, coral; d, discocycline; da, dasycladacean algae; g, gastropod; gc, geniculate coralline; he, hyaline encrusting foraminifer; m, miliolid; n, nummulite; oas, operculiniform assiline; or, orbitolite; os, ostracod; p, peloid; pl, planorbulinid; q, quartz; r, rotaliid; s, spirolinid; so, solenomerid.

lignite beds; Table 1, Fig. 5).

5.8. *Mf8 - Coral-foralgal boundstone (Table 2; Figs. 5, 6 and 7)*

This microfacies is represented only in the Harania section for a thickness of 6,5 m, and is included in the lithofacies F1 (algal limestones with flat large nummulites; Table 1, Fig. 5).

In the lower levels (Fig. 7, photo 7), the microfacies is constituted by a overall poorly-sorted coral-rhodalgal floatstone in a wackestone-to-packstone matrix, where some coral cobbles (2–3 mm) (15–20%), free-living small lumpy *Sporolithon* rhodoliths (up to 5 mm in diameter) (10–15%) and an incipient crustose coralline algal pavement are developed to form laminar (encrusting-to-foliose) thalli (10–15%), which bifurcate and join. Coral cobbles form coating structures wraped by the same encrusting foraminiferal assemblage (10%) described in the upper beds of the facies. The matrix presents common rotaliids (5%), udotacean *Ovulites* (5%), bryozoans (5%), textularids (3–5%), geniculate coralline remains (3–5%), cymbaloporid *Fabiania cassis* (2–3%), and occasionally, *Orbitolites*, miliolids, planktic foraminifers, ostracods, annelids, mollusk remains and echinoid debris.

In the upper levels this poorly- to moderately-sorted microfacies (Fig. 7, photo 8) shows a coral framestone-bindstone texture, with abundant colonial corals (20–25%). These are often wraped by crustose coralline algae (15–20%), hyaline foraminiferal encrusters (10–15%), and agglutinate *Haddonia heissigi* (2–3%) in multilayered red algae encrusting successions (Type 2 of Nebelsick and Bassi, 2000) with alternating thin layers of *Lithoporella melobesioides* and other crustose coralline, acervulinids (*Acervulina linearis*), planorbulinids (*Planorbulina* aff. *uva, P.* sp.) and homotrematids (*Miniacina multiformis, M.* sp.). Sometimes, bivalves boring the corals have been observed, and the matrix presents a packstone texture with abundant miliolids (10%), dasycladacean algae (5–10%), echinoid debris (5–10%) and peloids (5–10%). *Alveolina* (5%), *Orbitolites* (2–3%), cymbaloporid *Fabiania cassis* (2–3%), rotaliids (*Neorotalia* and *Gyroidinella* among others) (2–3%), textularids (2–3%), and ostracods (2–3%) are also common, and geniculate coralline segments, discorbids and planktic foraminifers are also present occasionally.

6. Depositional environment

In this section a paleoenvironmental interpretation based on the main litho- and microfacies features will be provided. The paleoenvironmental model adopted (Fig. 8) is based on the so-called 'distally-steepened ramp' proposed by Handford and Loucks (1993), but also using the ramp subdivision terminology according to Burchette and Wright (1992), but also considering the photic subdivisions according to Pomar (2001) and Pomar et al. (2017), so that the 'mesophotic zone' appears. In particular, the uppermost boundary of this mesophotic zone could coincide with the lower limit of the 'uppermost photic zone' of Hottinger (1997), near to the depth of 40 m and the deepest occurrence of marine vegetation (Pomar, 2001). The lowermost boundary could coincide with the lower limit of the 'upper photic zone' of Hottinger (1997), near the depth of 80 m, and coinciding with the dominance of orthophragminids in the LBF assemblage. Morphologic terminology used to describe samples with crustose coralline red algae is based on Nebelsick and Bassi (2000).

6.1. Inner ramp

This depositional environment is recognized from the microfacies *Mf1, Mf2* and *Mf4,* observed in the lower-middle portion of both Harania and Peñicas stratigraphic sections, and by the microfacies *Mf7* and *Mf8,* which were recognized only in the Harania section (Figs. 5 and 6).

The microfacies *Mf7* represents the most internal inner ramp, due to the presence of scattered miliolids, thin-walled ostracods, plant debris, oogonia and thallus of charophytes, as well as the laminae of silt and lignite interspersed in a general fine grain-sized sediment imply probably clastics contributions and flora remains from the nearby continent. All this suggests a very restricted shallow-marine to peritidal setting in eutrophic environments (Brasier, 1975; Wray, 1977; Flügel, 2010). This facies was interpreted as lagoonal to mangrove deposits with locally rich Nypa-bearing pollen associations (Kevdes et al., 1996; Solé de Porta et al., 2007).

The predominance of miliolids and peloids within a fine to medium grain-sized sediment with a moderately to well-sorted texture (microfacies *Mf4*), suggests a mesotrophic protected lagoon environment (Hallock et al., 1991; Murray, 2006; Amao et al., 2016). The abundance of fine-sized micritic grains (peloids) is the result of *syn-* to post-sedimentary reworking processes of weakly lithified carbonate mud in shallow marine conditions subjected to tide and wave action, especially in tropical settings (Flügel, 2010). Abundant porcelaneous foraminiferal tests, especially miliolids, indicate low turbulence warm water in restricted settings and, in turn, sligthly hypersaline conditions (Roozpeykar and Moghaddam, 2016; Chan et al., 2017; Sarkar, 2019). Common dasycladales, discorbids, rotaliids, thin-walled ostracods, and occasional remains of geniculate coralline algae, indicate warm water lagoonal marine environments with normal salinity (Brasier, 1975; Wray, 1977; Flügel, 2010). The presence of quartz grains suggests a proximity to the continent, which would have caused a siliciclastic supply by runoff a nutrient increase in the marginal marine waters, as well as sudden salinity changes in these extremely shallow marine environments. The poor bioclastic content observed locally, basically constituted by heterotrophic small benthic foraminifers (discorbids, miliolids, rotaliids, textularids and echinoid remains) could be explained by the formation of restricted conditions in upper sublittoral settings

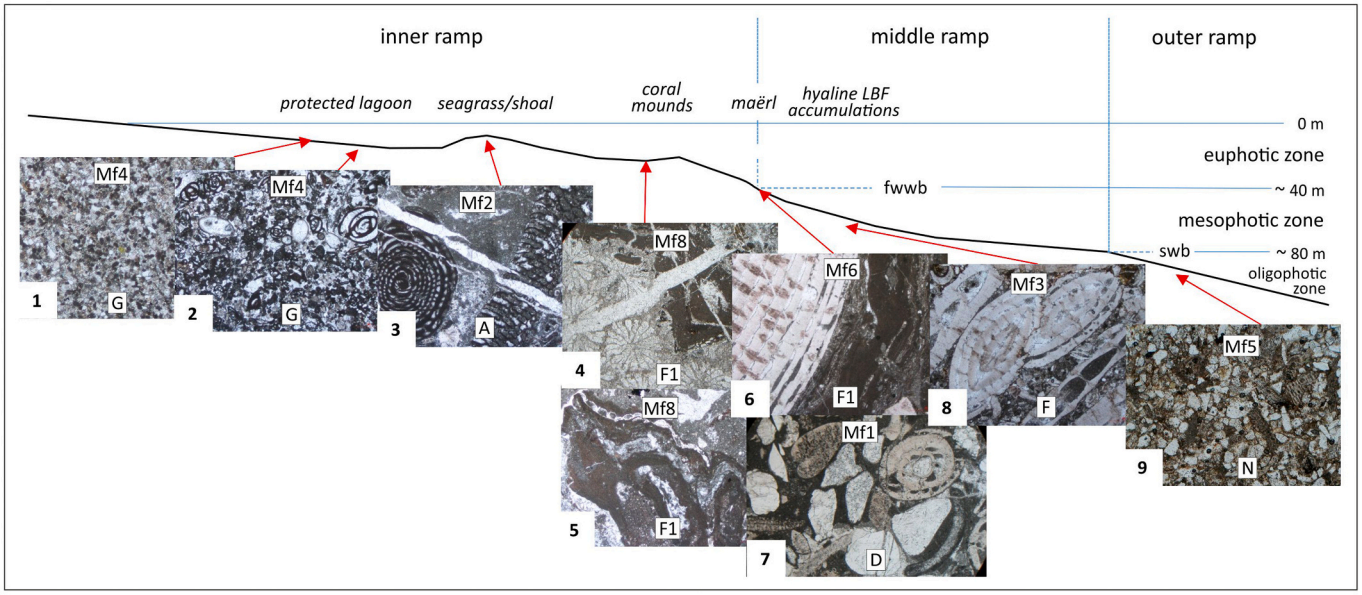

Fig. 8. Synthetic environmental microfacies interpretation for the Eocene marine Depositional Sequence in the Malaguide of Vélez-Rubio/Málaga sectors with location of facies and microfacies. 1–2 (Mf4) Protected inner ramp lagoon, subtidal environment; 3 (Mf2), Inner ramp seagrass/shoal, subtidal environment; 4–5 (Mf8), Coral-foralgal environment; 6 (Mf6), Nummulite-foralgal and 7 (Mf1) 'transgressive lag deposit' in the proximal middle ramp environment; 8 (Mf3), Middle ramp hyaline LBF accumulations (nummulitids); 9 (Mf5), Outer ramp environment. Ramp subdivision is based on Burchette and Wright (1992), and photic zones are after Hottinger (1997), Pomar (2001) and Pomar et al. (2017), modified.

(Brasier, 1975; Davaud and Septfontaine, 1995; Murray, 2006), occasionally influenced also by storm events that provide marine bioclasts to the coastal plain environments. Beavington-Penney et al. (2006) report an analogous microfacies model for the Middle Eocene deposits of Oman.

In the intermediate portion of the inner ramp the biotic association, which is mainly composed by porcelaneous LBF (alveolines and orbitolites), miliolids, dasycladacean algae, and rotaliids (microfacies *Mf2*), suggests a lagoonal environment with the presence of a conspicuous marine plant cover (seagrass meadows; Hottinger, 1997; Reich et al., 2015). Orbitolites, discorbids and some rotaliids are a common assemblage in seagrass inhabiting attached on the blades, thalli or rhizomes both in marine phanerogams and in smaller algae (Hottinger, 1983, 1997; Langer, 1993; Beavington-Penney et al., 2004; James and Bone, 2007; Mateu-Vicens et al., 2014; Reich et al., 2015; Tomás et al., 2016; Tomassetti et al., 2016; Brandano et al., 2019; Martín-Martín et al., 2021). Other small foraminifers (as miliolids and textularids), with motile and grazing life habit, are often found dwelling among rhizomes of marine vegetation (Langer, 1993; Perry and Beavington-Penney, 2005; Murray, 2006; Reuter et al., 2011; Mateu-Vicens et al., 2014). Green algae (dasycladales) often constitute an important element in shallow illuminated seafloors (Wray, 1977; Mateu-Vicens et al., 2014; Brandano et al., 2019). Alveolines, which are one of the main components, are often found trapped in this facies as rounded reworked grains, possibly as a result of waves and currents transport from neighboring inner ramp areas without vegetal cover (Spanicek et al., 2017). Likewise, many miliolids and rotaliids have suffered the same rolling and wear process. This microfacies can be associated to the green algal (GA)-foralgal assemblage according to Brandano et al. (2019), where the dominance of green algae and porcelaneous LBF on subordinate coralline algae could indicate low canopy seagrass meadows in tropical sea waters.

The distal zones of the inner ramp (microfacies *Mf8*) show common hermatypic corals with a related assemblage of coralline red algae, characterized by thin layers of *L. melobesioides* alternating with a diversified encrusting foraminifer association wraping the coral structure in multilayered and complex encrusting successions ('foralgal crusts', Bosellini and Papazzoni, 2003; 'coralline crusts', Bassi, 2005). These features suggest warm water and high-lightened conditions in shallow marine environments. *L. melobesioides* has been traditionally related to tropical and subtropical habitats (Wray, 1977; Bosence, 1983; Brandano et al., 2005; Roozpeykar et al., 2019; Li et al., 2021). The paleoecological comparison between the encrusting foraminiferal assemblage dominated by hyaline flat forms, and the analogous genus in recent associations seems to indicate a general shallow marine environment (Hottinger, 1983; Bosellini, 1998; White, 2002; Bosellini and Papazzoni, 2003; Nebelsick et al., 2005; Smith, 2015). Besides this, the agglutinated encrusting forms as *Haddonia heissigi* could indicate cryptic settings with subdued light conditions in the same environment (Matteucci, 1996; Rasser, 2000; Bosellini and Papazzoni, 2003). In the lower part of the Harania section, coralline crustose algae occur in the three following different modes: (a) "coralline coatings" on coral pebbles; (b) free-living lumpy rhodoliths (*Sporolithon*); and (c) lamellae (Nebelsick and Bassi, 2000), in layered-to-foliose coralline thalli. All these morphologies appear scattered on a medium to coarse-grained mobile substrate, but the lamellar morphology could represent the onset of stabilization and cementation of the sea-bottom (Taberner and Bosence, 1985; Basso, 1998; Bosellini and Papazzoni, 2003; Rasser and Piller, 2004; Basso et al., 2008). Also the presence of rotaliids, miliolids, textularids, dasycladales and *Fabiania* confirm the overall shallow marine conditions for this microfacies. From the trophic point of view, in recent environments the colonial hermatipic corals, like LBF, have a mixotrophic nutrition, which is highly advantageous in low-nutrient conditions, and therefore they preferably occupy oligotrophic habitats (Hallock, 2001; Hallock and Schlager, 1986; Mutti and Hallock, 2003; Pomar et al., 2017). Contrarily, coralline red algae and encrusting foraminifers, which are more dependent on available light, compete for space in oligotrophic to mesotrophic conditions (Adey and MacIntyre, 1973; Bosence, 1984; Hallock et al., 1991). The low occurrence of oligotrophic LBF (only a few alveolines and occasional orbitolites), and their replacement by small benthic foraminifers taxa and other heterotrophic biota, in addition to the conspicuous bioerosion observed in corals, indicate an increased nutrient supply and support mixed oligotrophic-mesotrophic conditions in a coral-reef environment (Hallock and Schlager, 1986; Mutti and Hallock, 2003).

Finally, the microfacies *Mf1* represents reworked deposits probably related to a transgressive phase including an important content of well-rounded quartz grains and pebbles within a packstone texture constituted by a mixed biogenic assemblage. This microfacies is also dominated by large benthic foraminifers from both internal (alveolinids) and middle ramp settings (nummulitids and orthophragminids) (Hottinger, 1997), and by other mainly shallow marine biota (miliolids, rotaliids, textularids, green algae and mollusks). The siliciclastic input, the mixed biotic association, and the stratigraphic position of the microfacies suggest sedimentation in not-specifiable inner ramp environments.

6.2. Middle ramp

This depositional setting is recognizable from the microfacies *Mf3* and *Mf6*. Both microfacies are dominated by accumulations of hyaline-LBZ tests (nummulitids, amphisteginids, rotaliids and orthophragminids), which are often wraped by crustose coralline algae and interlayered encrusting foraminifers in the *Mf6*. The well developed nummulite population marked by A and B-morphotypes (megalospheric and microspheric forms respectively, linked with the sexual evolutive stage) recognized in a packstone texture suggests an optimal habitat range at mesophotic and oligotrophic marine conditions in the middle ramp (Hottinger, 1997; Geel, 2000; Martín-Martín et al., 2020c, 2021). The "encrusting" growth of coralline algae, with flattened thalli on nummulite tests and fruticose branches observed, which indicate an environmental change from the conditions described above, mark the development of a mesotrophic maërl environment, where moderate bottom currents probably related to storm events can turn over tests to form rhodoliths (Rasser, 2000; Bassi, 2005; Nebelsick et al., 2013). The additional presence of a heterotrophic biotic assemblage (echinoid debris, small benthic foraminifers, annelids, bryozoans and ostreids) supports mesotrophic conditions (Hallock, 1988b; Hallock et al., 1991; Brasier, 1995) and does not rule out eventual nutrient input fluxes (Hallock, 1988a; Hottinger, 1997; Afzal et al., 2011). So, fine-sized quartz grains can be explained by the input of suspended debris supply from erosion of the hinterland, and some elements as discorbids, occasional orbitolites and dasycladales can be reworked down ramp from neighboring inner ramp areas during storm events.

6.3. Outer ramp

This depositional setting is only represented by the microfacies *Mf5*. The scarcity and low diversity of fossils, the absence of LBF and the common presence of planktic foraminifers suggest low luminosity habitats in open marine settings (Hallock and Glenn, 1986; Buxton and Pedley, 1989; Burchette and Wright, 1992; Romero et al., 2002; Flügel, 2010; Silva-Casal et al., 2019; Martín-Martín et al., 2021). The heterotrophic fossil assemblage constituted by small benthic foraminifers (bolivinids, unspecific rotaliids), fine-walled ostracods, small mollusk and echinoid remains indicates mesotrophic to eutrophic conditions (Wood, 1993; Brasier, 1995; Pomar, 2001; Mutti and Hallock, 2003; Pomar et al., 2017), which could be explained by high rates of primary production at the ocean surface. On the other hand, it can lead to low-oxygen conditions on the sea floor where only eutrophic benthic taxa may thrive (Mutti and Hallock, 2003). In this way, the dominance of bolivinid in sediments has been commonly related to low-oxygen sea-bottom conditions in outer shelf and upper bathyal settings (Lutze,

1964; Brasier, 1995; Obiosio, 2013; Khanolkar and Saraswati, 2019). Besides, the presence of common subangular fine-sized quartz grains indicates episodic periods of nutrient supply by means of turbidite currents triggered by storms and/or exceptional continental water flows induced by increased fluvial run-off (Brasier, 1995).

7. Discussion

7.1. Paleoenvironmental cycles and paleogeographic reconstruction

The Eocene sedimentary record in the Peñicas and Harania areas is only represented by Cuisian to middle Lutetian deposits arranged in a transgresive succession, and composed by several minor transgressive-regressive depositional cycles. This Eocene *p.p.* succession overlies Jurassic limestones (Peñicas section) and Paleocene deposits (Harania section) by means of an erosive surface (Fig. 5). In the Peñicas section the first depositional cycle is represented by a transgressive basal unit with a LBF-rich mixed assemblage of an inner-to-middle ramp environment. It is followed by an oligotrophic carbonate interval that passes from porcelaneous LBF-rich limestones deposited in inner ramp seagrass conditions, to nummulitid-rich limestones corresponding to a middle ramp environment. Finally, a peloidal quatzsiltite, which is characteristic of a restricted inner ramp environment, closes the cycle. In the Harania section, the succession is similar but the last nummulitid-rich interval is not represented, and the cycle ends with a miliolid and peloidal packstone/grainstone related to inner ramp protected lagoon settings followed by a last interval of marly pelites with lignite beds, which marks the transition to the continental realm.

The second depositional cycle (mostly lower Lutetian) consists of a nummulitid-rich limestone, which in the Peñicas section evolves to a quartzsiltitic interval with small bolivinids and planktic foraminifers of middle to outer ramp settings. In the Harania section, this second depositional cycle is represented by two intervals: the first one is made of a seagrass porcelaneous LBF-rich limestone, which passes to marly pelites with lignites in a transitional-to-continental context; the second one, consists of a coral-foralgal boundstone deposited in inner ramp settings.

In the Peñicas section the third depositional cycle (middle Lutetian), is only represented by a nummulite-foralgal packstone of proximal middle ramp environments. The environmental distribution of the recognized Early to Middle Eocene biotic assemblages is shown in Fig. 8, together with selected images of the described microfacies.

The Cuisian-Lutetian fossiliferous assemblage of the analyzed Peñicas and Harania sections shows a mixture of photozoan and heterotrophic elements. The photozoan association, constituted by abundant LBF, common green and red calcareous algae and some colonial corals, suggests euphotic to mesophotic conditions in oligotrophic marine warm-waters corresponding to low-middle latitudes. The heterotrophic assemblage, which is constituted by small benthic and planktonic foraminifera, mollusks, echinoids, bryozoans, annelids and other filter-feeding organisms occurs associated with photozoan components, or isolated from the latter as a unique association, suggesting availability of nutrients in meso- to eutrophic habitats related to neighboring upwelling settings or from terrestrial clastic supply. In any case, the overall recognized fossiliferous assemblage is arranged in characteristic marine belts distributed in mobile mosaics (sensu Wright and Burgess, 2005). These belts deepen from the innermost marine environments to the open marine settings of the outer ramp. The euphotic inner ramp settings are characterized by oligo- to mesotrophic conditions, characterized by marine vegetation (seagrass) and/or coral-rich settings. Mesophotic middle ramp environments are represented mainly by oligotrophic nummulitid-rich deposits, which can evolve to mesotrophic maërl settings. Oligophotic outer ramp environments are characterized by meso-eutrophic bolivinid and planktonic foraminifera-rich quartzsiltites suggesting temporary steps of nutrient availability as a result of hydraulic discharges and detrital supply from the hinterland rivers, without ruling out the presence of neighboring upwelling settings. From the carbonate *"factory"* point of view, the model here proposed is analogous to that described by Buxton and Pedley (1989) and Flügel (2010) and can also be compared to the warm temperate province of Betzler et al. (1997), especially to the heterozoan warm water carbonates of Westphal et al. (2010). As reported by these authors, the fossiliferous assemblage shows a transition from photozoan to heterozoan carbonates, in particular moving to outer marine ramp settings where the concentration of nutrients appears to increase. Furthermore, various proxies proposed by Westphal et al. (2010) for the recognition of this type of carbonate factory in the fossil record have also been observed in our work. Carbonate grain associations, with a mixture of autotrophic (coralline and green algae), mixotrophic (LBF, corals) and heterotrophic components (mollusks, echinoids, bryozoans, small benthic and planktic foraminifers) could point to warm temperatures and high nutrient conditions. From the paleoceanographic point of view, also the presence of siliciclastic silt grains in distal environments could indicate upwelling settings, regional current patterns, fluvial influx from hinterland or dust supply. Our data can also be related to the 'oligo-mesotrophic, warm-temperate system characterized by red algal and seagrass derived biota' proposed by Michel et al. (2018), and in particular to the 'type 5, warm-temperate, oligotrophic, distally steepened ramp' of their depositional model for the distribution of heterozoan carbonates.

A paleogeographic 3D reconstruction is shown in Fig. 9, where paleoenvironments are displayed laterally for the whole Middle Eocene according to the Walter Law rules.

7.2. Eocene carbonate platforms of the westernmost Tethys and comparison with other Tethyan sectors

The Ypresian-Lutetian paleoenvironmental evolution reconstructed for the studied area has been compared to other Tethyan sectors (Fig. 1B), with the aim to verify general constraints for the evolution of the Western Tethyan platforms in the considered time span.

7.2.1. Betic and Rifian sectors

Eocene shallow marine deposits are widely known in the Betic Cordillera, as well as in the Rif, although few detailed studies have been performed.

The Eocene sedimentary record in the External Betic Zones, which represents platform deposits in the Southern Iberian Margin, is mainly represented in the Alicante (Penaguila-Ibi-Onil sections [Pb: Fig. 1B], Geel, 2000; Ascoy section, Höntzsch et al., 2013) and Murcia areas (El Carche-Jumilla-Cieza sections; Kenter et al., 1990; Chacón and Martín-Chivelet, 2005). The latter is generally characterized by shallowing-upwards carbonate successions controlled by tectonics and relative sea-level changes.

The sedimentary record of the Ypresian-Lutetian transition is only documented in the Onil section (Geel, 2000). Even if the proposed age is inaccurate, the section shows a marked regressive depositional trend, which evolves from inner-to-middle ramp environments (Ypresian) in restricted marine settings (Lutetian). This sedimentation passes southwards to slope and deep marine facies: (1) the Alicante Peñas Montesas-Villafranqueza-Amadorio-Busot-Pantanet (Guerrera et al., 2006) and Agost sections (Molina et al., 2000); (2) the Fortuna area in the Murcia region (Kenter et al., 1990; Ortiz and Thomas, 2006). No corals are reported in these areas.

The shallow-marine Eocene sedimentary record in the Internal Betic Zones, which corresponds to platform deposits in the southwestern part of the Mesomediterranean Microplate, is represented by the Malaguide Complex (Ma: Fig. 1B) and its equivalent Ghomaride Complex, together with the Internal Dorsale (Frontal Units) in the Rif (Ri: Fig. 1B). The most complete Eocene successions are developed in the eastern Malaguide units of Sierra Espuña area (SE Spain), which show a continuous Upper Ypresian (Cuisian) to Bartonian (SBZ10–18) stratigraphic record. In this area the Ypresian-Lutetian transition shows a shallowing-

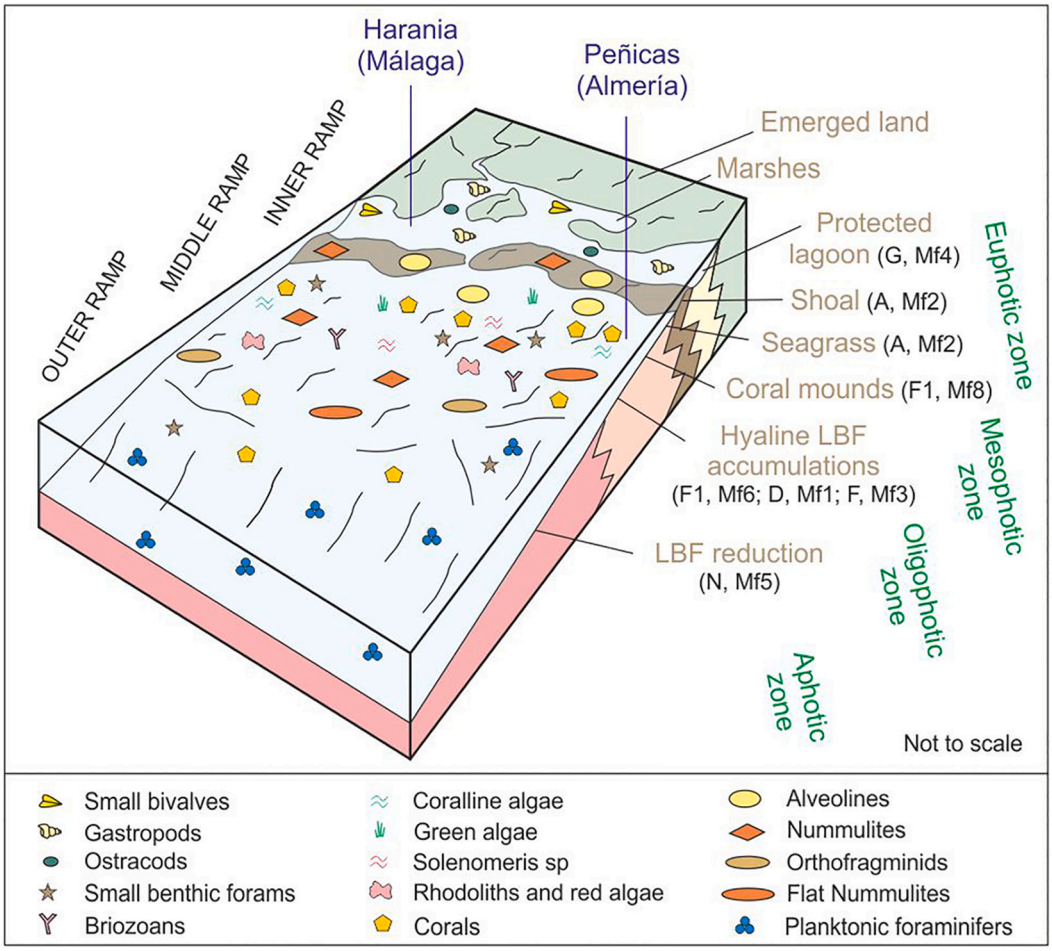

Fig. 9. Paleogeographic and paleoenvironmental 3D-sketch model of the Central-Western Malaguides with location of facies and microfacies during the Eocene.

upwards trend, which evolves from inner-middle ramp environments to restricted marine and continental settings in the Prado Mayor and Malvariche sections, where some small z-coral buildups have been recorded in the early Cuisian (SBZ10) deposits (Martín-Martín et al., 2020c, 2021).

In the central and western Malaguides (here studied) the Eocene stratigraphic record shows a much more fragmentary and discontinuous character than in the eastern Malaguides, the latter studied by Martín-Martín et al. (2020c, 2021). At present, it is difficult to verify if this is due to the lithostratigraphic omission related to tectonic effects and/or to the presence of sedimentary hiatuses, because only the lower-middle Cuisian (SBZ 10–11?) and lower-middle Lutetian (SBZ 13–14) deposits have been recognized in this area. Also the absence of LBF in the marly beds, which did not lead to a realiable dating, could be responsible for the impossibility of recognizing some of the late Ypresian biozones, instead well characterized in the Sierra Espuña area. This sedimentary succession is very condensed and indicates inner marine environments in the Harania section, while it is better developed in the Peñicas section where it shows a more open marine realm. In both sections the Cuisian deposits show a shallowing-upwards trend from middle to protected inner ramp settings (Peñicas) to restricted inner ramp lagoon environments (Harania). In the Harania section, the Lutetian succession evolves from an inner ramp setting to a middle ramp environment. The Peñicas section upwardly shows middle to outer ramp settings followed by inner-middle ramp conditions. In the inner ramp of the Harania section colonial corals have been recognized.

In the westernmost Malaguide Complex, Maaté et al. (2000) pointed out equivalent carbonate successions outcropping in the Ardales and Gaucín areas (western Malaga province), characterized by a similar shallowing-upwards sequence composed of lower-middle Cuisian (SBZ10–11) LBF-rich limestones, which unconformably lie above a Jurassic substrate. No corals were reported in these areas by these authors.

In the northern Morocco, the Ghomaride Domain (Ri: Fig. 1B) is also an element to be considered to understand the lack of continuity in the Eocene sedimentary record. The marly levels interbedded in the carbonate sequence can act as detachment/decollement levels for the different superimposed nappes, whose evolution reduced certain sedimentary sections and repeated other ones. In the locality of Aïn Boukhalfa Maaté et al. (2000) an Eocene succession constituted by a LBF-rich sandy limestone and a limestone unit with coralline algae and LBF (lower-middle Cuisian; SBZ10–11), unconformably lying above a Jurassic to Paleocene substrate has been pointed out. Contemporary deposits have also been described (Maaté et al., 2000) at the localities of Oued el Gharraq and Oued el Lile, in the Rifian internal Dorsale. In the first section (Oued el Gharraq), a Paleocene unit (Danian: SBZ1) is unconformably covered by a lower-middle Cuisian (SBZ10–11) LBF-rich limestone succession. The Oued el Lile is the most complete section in this area and it is characterized by four stratigraphic levels extending from Paleocene to middle Lutetian. In this section, the Eocene succession consists of a transgressive sequence that begins with a sandy limestone interval, with alveolines and glauconite, topped by micritic LBF-rich limestones. Both intervals are lower-middle Cuisian (SBZ10–11). The section is characterized upwards by a middle Lutetian (SBZ14) LBF-rich calcarenitic interval and a planktonic foraminifers-rich upper marly bed, referable to an imprecise middle Lutetian age. Late Cuisian (SBZ12) and

early Lutetian (SBZ13) zones are believed to be either greatly reduced or absent in this area. No corals are reported by the mentioned authors in the Ghomaride Complex.

In short, the Harania section (shallow-water conditions) is similar to the Ardales and Gaucín sections, of the western Malaga province and to those of the Aïn Boukhalfa and Oued el Gharraq in the Moroccan Rif. Instead the Peñicas section (deeper water conditions) shows correlation with the Moroccan Rif Oued el Lile section (Maaté et al., 2000). The comparison of the Sierra Espuña area (Martín-Martín et al., 2020c, 2021) with the studied successions points out similar features: Harania and Prado Mayor; Peñicas and Castillo de Mula or Malvariche sections. The main difference is that the Sierra Espuña succession is more complete showing in some cases deeper realms. Corals are reported in the Harania sector (where the inner ramp is well developed) and in the Sierra Espuña area (Martín-Martín et al., 2020c, 2021), in contrast to the other Betic-Rifian sectors where no z-corals are mentioned.

7.2.2. Other Tethyan sectors

A shallow-marine sedimentation is widely developed during the Ypresian-Lutetian times both on the northern and southern belts of the Tethys, at paleolatitudes ranging from 40°N to near 10°S.

In the northern belt of the Tethys, extensive LBF-rich carbonate ramps dominate these environments, where broad LBF-rich platforms developed from the Pyrenean realm to the Tibetan sector, across Alps, Adriatic Platform, Apennines, Carpathians, Caucasus, Hellenian, Anatolian and Indian domains, at paleolatitudes between 35 and 45°N (Martín-Martín et al., 2001; Höntzsch et al., 2013; Martín-Martín et al., 2020c, 2021). Coral reef buildups, which florished and dominated shallow-marine environments mainly during the Paleocene and Middle Eocene, show a decline in abundance and diversity during most of the warm Ypresian EECO, due to excessively high temperatures, which shifted their occurrence to marginal environments (Scheibner and Speijer, 2008; Vescogni et al., 2016; Pomar et al., 2017). The few citations reported about their Late Ypresian occurrence refer to the 'post-EECO cooling' event recognized in the uppermost Middle Cuisian (SBZ11) deposits of the Monte Postale (Lessini shelf, NE Adriatic platform, NE Italy; Vescogni et al., 2016). During the early Lutetian, which is characterized by the same cooling period, several coral patch-reefs and z-coral debris have been reported from several localities of the Pyrenees (Pi: Fig. 1B). Here small coral-buildups have been recognized in the early Lutetian (SBZ13) of Sierras Exteriores in the Mediano anticline (Poblet et al., 1998) and Isuela section (Rodríguez-Pintó et al., 2012). The z-coral record has been also reported from the Adriatic Platform. In this area scattered coral debris of an imprecise Ypresian-Lutetian age has been described in the western Istria deposits (Maticec et al., 1996), in the lower-middle Lutetian deposits of the middle Adriatic Croatia offshore (Kovacic, 1997), and in the lower Lutetian limestone blocks reworked as younger sediments in the W Herzegovina platform (Dragicevic et al., 1992).

LBF carbonate platforms developed on the southern Tethyan margin between Morocco (Mo: Fig. 1B) and the Oman-Yemen domains at paleolatitudes ranging from 20°N and the equator (Höntzsch et al., 2013; Martín-Martín et al., 2020c, 2021). No z-corals oldest than middle Lutetian have been reported in this realm. The main periods of coral growth occurred during the warm periods of the Middle Eocene (LLTM and MECO events, at late Lutetian-Bartonian times, SBZ16–17). This growth was mainly restricted to the eastern sector (ie, northern Egypt and Arabian domains) where the nutrient-enriched waters did not affect biotic assemblages of shallow-marine environments (Martín-Martín et al., 2021, and references therein). In the southern Tethyan Margin the Ypresian-early Lutetian interval is mainly represented by wide LBF-rich ramps, where especially nummulite-bank buildups thrived (Racey, 2001; Jorry et al., 2006). The Middle-Upper Eocene deposits are missing at the top of the upper Ypresian El Garia and Jdeir formations, in the marine platforms of central Tunisia (Tu: Fig. 1B) and NW Libya, respectively. An increasing eutrophication of shallow marine waters is constated in these domains as a result of the detrital contribution (Bernasconi et al., 1991; Loucks et al., 1998; Racey, 2001; Jorry et al., 2006). During this time-span an analogous tectono-sedimentary activity has been also documented in the platform areas of Saudi Arabia, United Arab Emirates, Qatar, Kuwait, Iraq, Jordan and Palestine (Anan, 2010, and references therein).

In short, the widespread distribution of LBF during the Early Eocene leads to the disappearance or extreme reduction of coral constructions (Martín-Martín et al., 2020c). Nevertheless, abundant corals have been observed in the Cuisian beds of the Sierra Espuña (Martín-Martín et al., 2020c, 2021) and also in the Harania section, in both cases associated with inner ramp realms. This indicates that corals could continue to develop in the westernmost Tethys at 35° N and 0° to 5°E (Eocene coordinates), in contrast to other Tethyan areas. The Ypresian-early Lutetian time-span is a period of transition for global temperature, tectonic activity, and sea-level curve, which affected ecologic parametres and biotic assemblages developed in shallow-marine environments. So, during this period LBF-rich belts covered the euphotic-mesophotic carbonate marine ramps in oligotrophic settings, and z-corals only thrived locally where optimal ecologic conditions made it possible. This occurs preferably in marginal settings as in the eastern and central sectors of the Malaguide Complex in the internal Betic realm (Martín-Martín et al., 2021, and this work).

8. Conclusions

The Peñicas (Almería) and Harania (Málaga) Eocene stratigraphic sections from the Malaguide Complex in the Betic Cordillera (at about 35°N and 0° to 5°E, according to the Eocene coordinates) and belonging to the westernmost Tethys have been studied. In the mentioned sections the Eocene succession is represented by Cuisian (SBZ 10) to middle Lutetian (SBZ 14) deposits (Fig. 10).

In the Peñicas and Harania sections the lithofacies A, B, D, F, F1, F2, G, M, N and R were recognized. These lithofacies represent shallow marine platform realms. On the basis of the fossiliferous assemblage, texture and fabric, eight microfacies were also recognized and named from ***Mf1*** to ***Mf8***, according to the first appearance. In the Harania section the Eocene succession shows an evolution from an inner ramp setting to a middle ramp environment, while in the Peñicas section an evolution from middle to outer ramp settings, which finally return to inner-middle ramp conditions, has been recognized. In addition, colonial corals have been observed in the inner ramp.

The Eocene deposits are arranged into a transgressive succession constituted by three minor transgressive-regressive sedimentary cycles. (1) The first one (mostly Cuisian) is represented by a transgressive basal unit containing LBF-rich mixed assemblage from inner-to-middle ramp environments. This cycle is followed by an oligotrophic carbonate interval, where porcelaneous LBF-rich limestones, which deposited in inner ramp seagrass or protected lagoon conditions, pass to nummulitid-rich limestones of a middle ramp environment. (2) The second cycle (mostly lower Lutetian) is made of a nummulitid-rich limestone (sometimes seagrass porcelaneous LBF), which in the Peñicas section evolves to a quartzsiltitic interval with small bolivinids and planktic foraminifers in middle to outer ramp settings. In the Harania section this second cyle consists of clays with lignite (marshy or lagoonal realm) which show a transition to coral-foralgal boundstone in inner ramp settings. (3) The third depositional cycle (middle Lutetian) is only represented in the Peñicas section consisting in a nummulite-foralgal packstone in proximal middle ramp environments.

The fossiliferous assemblage analyzed in the Cuisian-Lutetian deposits shows a mixture of photozoan (LBF, green and red calcareous algae and corals) and heterotrophic (mollusks, echinoids, bryozoans, small benthic and planktic foraminifers) elements, suggesting euphotic to mesophotic conditions in oligo-mesotrophic marine warm-waters (Fig. 10) located at low-middle latitudes. It also indicates a transition from photozoan to heterozoan carbonates, in particular towards outer

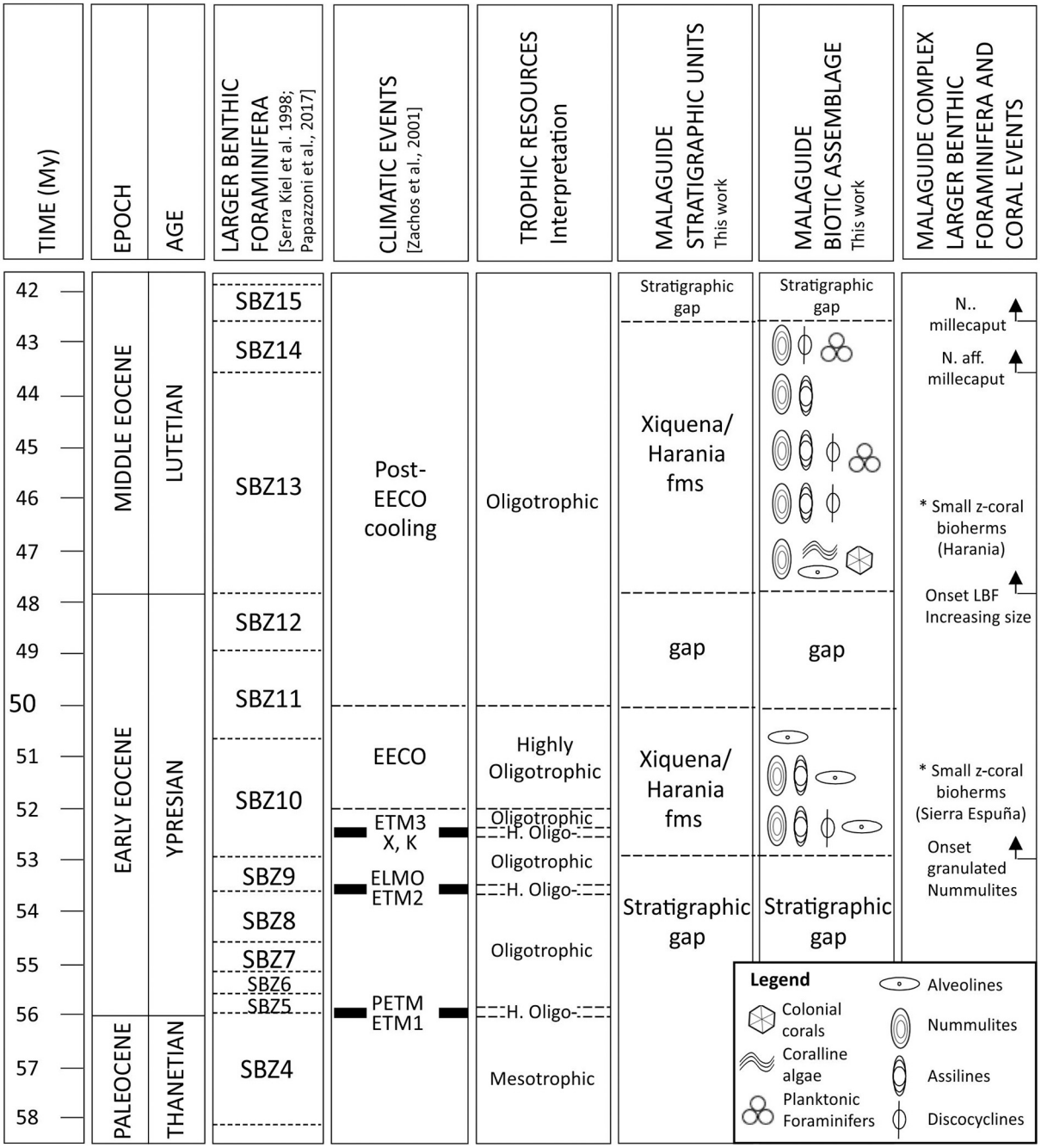

Fig. 10. Biochronostratigraphic chart of the Early-Middle Eocene including numerical time scale, epochs, ages, LBF zonation (SBZ), main climatic events, trophic resources interpretation, circum-Tethyan platfom stages, stratigraphic units in the Eastern Malaguides (Sierra Espuña), and stratigraphic units, biotic assemblages and main LBF and coral events in the studied central-eastern Malaguide Complex (Vélez Rubio) and western Malaguide Complex (Harania sections). Key: PETM (Paleocene-Eocene Thermal Maximum), ETM-1, ETM-2, ETM-3 (Eocene Thermal Maximum −1 to −3), X, K (Post- ETM-3 hyperthermal events), ELMO (Eocene Layer of Misterious Origin), EECO (early Eocene climatic optimum).

marine ramp settings.

In the central (Almería) and western (Málaga) Malaguides the Eocene record shows a much more fragmentary and discontinuous character than in the eastern Malaguides (Sierra Espuña). The Harania section is very condensed and represents an inner marine environment, while the Peñicas section is better developed and shows a more open marine character.

During the Early Eocene, the widespread distribution of LBF leads to the disappearance or extreme reduction of coral constructions. Nevertheless, abundant corals have been observed in the Harania section (Fig. 10) and in the Eocene beds of the Sierra Espuña, associated with inner ramp realms. This indicates that corals could continued to develop in the westernmost Tethys at about 35° N and 0° to 5°E according the Eocene coordinates (transition area to the Atlantic Ocean), in contrast to other Tethyan sectors. The Ypresian-Lutetian time-span is a period of transition in global temperature conditions, and corals only survived locally due to optimal ecologic conditions occurring preferably in marginal settings, as it seems to happen in the eastern and central sectors of the Malaguide Complex (internal Betic realm).

Declaration of Competing Interest

None.

Acknowledgements

Research supported by: Research Project PID2020-114381GB-I00, Spanish Ministry of Education and Science; Research Groups and Projects of the Generalitat Valenciana, Alicante University (CTMA-IGA). Grants from University of Urbino to F. Guerrera. We also thank Prof. Agustín Martín-Algarra and an anonymous reviewer for the very useful revision fournished.

References

Adams, C.G., Lee, D.E., Rosen, B.R., 1990. Conflicting isotopic and biotic evidence for tropical seasurface temperatures during the Tertiary. Palaegeogr. Palaeoclimatol. Palaeoecol. 77, 289–313.
Adey, W.H., MacIntyre, I.G., 1973. Crustose coralline algae: a reevaluation in the geological sciences. Geol. Soc. Am. Bull. 84, 883–904.
Afzal, J., Williams, M., Leng, M.J., Aldridge, R.J., 2011. Dynamic response of the shallow marine benthic ecosystem to regional and pan-Tethyan environmental change at the Paleocene-Eocene boundary. Palaeogeogr. Palaeoclimatol. Palaeoecol. 309, 141–160.
Agnini, C., Macri, P., Backman, J., Brinkhuis, H., Fornaciari, E., Giusberti, L., Luciani, V., Rio, D., Sluijs, A., Speranza, F., 2009. An early Eocene carbon cycle perturbation at ~52.5 Ma in the Southern Alps: Chronology and biotic response. Paleoceanography 24, PA2209.
Amao, A.O., Kaminski, M.A., Setoyama, E., 2016. Diversity of foraminifera in a shallow restricted lagoon in Bahrain. Micropaleontology 62, 197–211.
Anan, H.S., 2010. A stratigraphic lacuna around the Ypresian/Lutetian boundary (Early-Middle Eocene) in Arabia and other localities in the Tethys. J. Al Azhar Univ. Gaza (ICBAS, Special Issue) 12, 11–18.
Bassi, D., 2005. The Upper Eocene crustose coralline algal pavement in the Colli Berici, north-eastern Italy. Annali dell'Università di Ferrara Mus Sci Nat 1, 63–73.
Basso, D., 1998. Deep rhodolith distribution in the Pontian Islands, Italy: a model for the paleoecology of a temperate sea. Palaeogeogr. Palaeoclimatol. Palaeoecol. 137, 173–187.
Basso, D., Vrsaljko, D., Grgasović, T., 2008. The coralline flora of a Miocene maërl: the Croatian Litavac. Geol. Croatica 61, 333–340.
Beavington-Penney, S.J., Wright, V.P., Woelkerling, W.J., 2004. Recognising macrophyte-vegetated environments in the rock record: a new criterion using 'hooked' forms of crustose coralline red algae. Sediment. Geol. 166, 1–9.
Beavington-Penney, S.J., Wright, V.P., Racey, A., 2006. The Middle Eocene Seeb Formation of Oman: an investigation of acyclicity, stratigraphic completeness, and accumulation rates in shallow marine carbonate settings. J. Sediment. Res. 76 (10), 1–25.
Bernasconi, A., Poliani, G., Dakshe, A., 1991. Sedimentology, petrography and diagenesis of Metlaoui Group in the offshore Northwest of Tripoli. In: Salem, M.J., Belaid, M.N. (Eds.), The Geology of Libya, 2nd Symposium on the Geology of Libya. Tripoli, Libya, pp. 1907–1928.
Betzler, C., Brachert, T.C., Nebelsick, J., 1997. The warm temperate carbonate province. A review of the facies, zonations, and delimitations. Cour. Forsch.-Institute Senckenberg 201, 83–99.
Bosellini, F.R., 1998. Diversity, composition and structure of Late Eocene Shelf-edge coral associations (Nago Limestone, northern Italy). Facies 39, 203–226.
Bosellini, F.R., Papazzoni, C.A., 2003. Palaeoecological significance of coral-encrusting foraminiferan associations: a case-study from the Upper Eocene of northern Italy. Acta Palaeontol. Pol. 48 (2), 279–292.
Bosence, D.W.J., 1983. The occurrence and ecology of recent rhodoliths - A review. In: Peryt, T.M. (Ed.), Coated Grains, Springer-Verlag, Berlin, Ch, III-2, pp. 226–242.
Bosence, D.W.J., 1984. Construction and preservation of two recent coralline algal reefs, St. Croix. Caribbean. Palaeontol. 27, 549–574.
Brandano, M., Vannucci, G., Pomar, L., Obrador, A., 2005. Rhodolith assemblages from the lower Tortonian carbonate ramp of Menorca (Spain): environmental and paleoclimatic implications. Palaeogeogr. Palaeoclimatol. Palaeoecol. 226 (3), 307–323.
Brandano, M., Tomassetti, L., Mateu-Vicens, G., Gaglianone, G., 2019. The seagrass skeletal assemblage from modern to fossil and from tropical to temperate: Insight from Maldivian and Mediterranean examples. Sedimentology 66, 2268–2296.
Brasier, M.D., 1975. The ecology and distribution of recent foraminifera from the reefs and shoals around Barbuda, West Indies. J. Foraminifer. Res. 5, 193–210.
Brasier, M.D., 1995. Fossil indicators of nutrient levels. 1: Eutrophication and climatic change. In: Bosence, D.W.J., Allison, P.A. (Eds.), Marine Palaeoenvironmental Analysis from Fossils, 83. Geol. Soc. Spec. Publ, pp. 113–132.
Burchette, T.P., Wright, V.P., 1992. Carbonate ramp depositional systems. Sediment. Geol. 79, 3–57.
Buxton, M.W.N., Pedley, H.M., 1989. Short Paper: a standardized model for Tethyan Tertiary carbonate ramps. J. Geol. Soc. Lond. 146, 746–748.
Chacón, B., Martín-Chivelet, J., 2005. Subdivisión litoestratigráfica de las series hemipelágicas de edad Coniaciense-Thanetiense en el Prebético Oriental (SE de España). Rev. Soc. Geol. Esp. 18 (1–2), 3–20.
Chan, S.A., Kaminskia, M.A., Al-Ramadana, K., Babalolaba, L.O., 2017. Foraminiferal biofacies and depositional environments of the Burdigalian mixed carbonate and siliciclastic Dam Formation, Al-Lidam area, Eastern Province of Saudi Arabia. Palaeogeogr. Palaeoclimatol. Palaeoecol. 469, 122–137.
Critelli, S., Martín-Martín, M., Capobianco, W., Perri, F., 2020. Sedimentary history and palaeogeography of the Cenozoic clastic wedges of the Malaguide Complex, Internal Betic Cordillera, southern Spain. Mar. Pet. Geol. 124, 104775.
Davaud, E., Septfontaine, M., 1995. Post-mortem onshore transportation of epiphytic foraminifera: recent example from the Tunisian coastline. J. Foraminifer. Res. A65 (1), 136–142.
Dragicevic, I., Blaskovic, I., Tisljar, J., Benic, J., 1992. Stratigraphy of Paleogene Strata within the Mesihovina - Rakitno Area (Western Herzegovina). Geol. Croatica 45, 25–52.
Embry, A.F., Klovan, J.E., 1971. A Late Devonian reef tract on Northeastern Banks Island, NWT. Can. Petrol. Geol. Bull. 19, 730–781.
Flügel, E., 2010. Microfacies of carbonate rocks. In: Analysis, Interpretation and Application. Springer, p. 976.
Geel, T., 1973. The geology of the Betic of Malaga, the Subbetic and the zone between these two units in the Vélez Rubio area (Southern Spain). GUA Pap. Geol. 5, 191.
Geel, T., 2000. Recognition of stratigraphic sequences in carbonate platform and slope deposits: empirical models based on microfacies analysis of Paleogene deposits in southeastern Spain. Palaeogeogr. Palaeoclimatol. Palaeoecol. 155, 211–238.
Guerrera, F., Martín-Martín, M., 2014. Geodynamic events reconstructed in the Betic, Maghrebien and Apennine chains (central-western Tethys). Bull. Soc. Géol. France 185 (5), 329–341.
Guerrera, F., Martín-Martín, M., Perrone, V., Tramontana, M., 2005. Tectono-sedimentary evolution of the southern branch of the western Tethys (Magrebian Flysch basin and Lucanian Ocean). Terra Nova 17, 358–367.
Guerrera, F., Estévez, A., López-Arcos, M., Martín-Martín, M., Martin-Pérez, J.A., Serrano, F., 2006. Paleogene tectonosedimentary evolution of the Alicante Through (External Betic Zone, SE Spain) and its bearings on the timing of the deformation of the South-Iberian Margin. Geodin. Acta 19, 87–101.
Guerrera, F., Martín-Martín, M., Tramontana, M., 2021. Evolutionary geological models of the central-western peri-Mediterranean chains: a review. Int. Geol. Rev. 63 (1), 65–86.
Hadi, M., Less, G., Vahidinia, M., 2019. Eocene larger benthic foraminifera (alveolinids, nummulitids, and orthophragmines) from the eastern Alborz region (NE Iran): taxonomy and biostratigraphy implications. Rev. Micropaleontol. 63, 65–84.
Hallock, P., 1988a. Diversification in algal symbiont-bearing foraminifera: a response to oligotrophy. Rev. Paléobiol. spéc. 2 (Benthos'86), 789–797.
Hallock, P., 1988b. The role of nutrient availability in bioerosion: consequences to carbonate buildups. Palaeogeogr. Palaeoclimatol. Palaeoecol. 63, 275–291.
Hallock, P., 2001. Coral reefs, carbonate sedimentation, nutrients, and global change. In: Stanley, G.D. (Ed.), The History and Sedimentology of Ancient Reef Ecosystems. Kluwer Academic/Plenum Publishers, pp. 387–427.
Hallock, P., Glenn, E.C., 1986. Larger foraminifera: a tool for paleoenvironmental analysis of Cenozoic carbonate depositional facies. Palaios 1, 55–64.
Hallock, P., Schlager, W., 1986. Nutrient excess and the demise of coralreefs and carbonate platforms. Palaios 1, 389–398.
Hallock, P., Premoli-Silva, I., Boersma, A., 1991. Similarities between planktonic and larger foraminiferal evolutionary trends through Paleogene paleoceanographic changes. Palaeogeogr. Palaeoclimatol. Palaeoecol. 83, 49–64.
Handford, C.R., Loucks, R.G., 1993. Carbonate depositional sequences and systems tracts - responses of carbonate platforms to relative sea-level changes. In: Loucks, B., Sarg, R.J. (Eds.), Carbonate Sequence Stratigraphy: Recent Developments and Applications, 57. Am. Assoc. Petrol. Geol. Bull., pp. 3–41
Herbig, H.G., Trappe, J., 1994. Stratigraphy of the Subatlas Group (Maastrichtian-Middle Eocene, Morocco). Newsl. Stratigr. 30 (3), 125–165.
Hlila, R., Maaté, A., Sanz de Galdeano, C., Serra-Kiel, J., Serrano, F., El Kadiri, Kh., 2007. La serie paleógena de la unidad superior del Gomáride en Talembote (Rif Interno, Marruecos). Geogaceta 43, 91–94.
Höntzsch, S., Scheibner, C., Brock, J.P., Kuss, J., 2013. Circum-Tethyan carbonate platform evolution during the Palaeogene: the Prebetic platform as a test for climatically controlled facies shifts. Turk. J. Earth Sci. 22, 891–918.
Hottinger, L., 1983. Processes determining the distribution of larger foraminifera in space and time. Utrecht Micropaleontol. Bull. 30, 239–253.
Hottinger, L., 1997. Shallow benthic foraminiferal assemblages as signals for depth of their deposition and their limitations. Bull. Soc. Géol. France 168 (4), 491–505.
Jabaloy-Sánchez, A., Martín-Algarra, A., Padrón-Navarta, J.A., Martín-Martín, M., Gómez-Pugnaire, M.T., Sánchez-Vizcaíno, V.L., Garrido, C.J., 2019. Lithological successions of the internal zones and flysch trough units of the betic chain. In: Quesada, C., Oliveira, J.T. (Eds.), The Geology of Iberia: a Geodynamic Approach, Regional Geology Reviews. Springer Nature, Switzerland, pp. 377–432.
James, N.P., Bone, Y., 2007. A late Pliocene-early Pleistocene, inner shelf, subtropical, seagrass-dominated carbonate: Roe Calcarenite, Great Australien Bight, Western Australia. Palaios 22, 343–359.
Jorry, S., Davaud, E., Caline, B., 2006. Controls on the distribution of nummulite facies: a case study from the Late Ypresian el Garia Formation (Kesra Plateau, Central Tunisia). J. Pet. Geol. 26, 283–306.
Kazmer, M., Dunkl, I., Frisch, W., Kuhlemann, J., Ozsvart, P., 2003. The Paleogene forearc basin of the Eastern Alps and Western Carpathians: subduction, erosion and basin evolution. J. Geol. Soc. London 60, 413–428.
Kennett, J.P., Stott, L.D., 1991. Abrupt deep-sea warming, palaeoceanographic changes and benthic extinctions at the end of the Palaeocene. Nature 353 (6341), 225–229.

Kenter, J.A.M., Reymer, J.J.G., van der Straaten, H.C., Peper, T., 1990. Facies patterns and subsidence history of the Jumilla-Cieza region (southeastern Spain). Sediment. Geol. 67, 263–280.
Kevdes, M., Solé de Porta, N., Martín-Algarra, A., 1996. Spores and pollen grains from Eocene layers of Malaga, Spain. Plant Cell Biol. Devlop. 7, 37–55.
Khanolkar, S., Saraswati, P.K., 2019. Eocene foraminiferal biofacies in Kutch Basin (India) in context of palaeoclimate and palaeoecology. J. Palaeogeogr. 8, 21.
Kovacic, V.T., 1997. The development of the eocene platform carbonates from wells in the Middle Adriatic Off-Shore Area. Croatia. Geol. Croat. 50 (1), 33–48.
Langer, M.R., 1993. Epiphytic foraminifera. Mar. Micropaleontol. 20, 235–265.
Langer, M.R., Hottinger, L., 2000. Biogeography of selected larger foraminifera. Micropaleontology 46 (Supplement 1), 105–126.
Li, Y., Yu, K., Bian, L., Fan, T., Wang, R., Jiang, W., Xu, S., Zhang, Y., Yang, Y., 2021. Paleo-water depth variations since the Pliocene as recorded by coralline algae in the South China Sea Yinqiang. Palaeogeogr. Palaeoclimatol. Palaeoecol. 562, 110107.
Loeblich, A.R., Tappan, H.P., 1987. Foraminiferal genera and their classification. Van Nostrand Reinhold Company 2 vol, 970.
Loucks, R.G., Moody, R.T.J., Bellis, J.K., Brown, A.A., 1998. Regional depositional setting and pore network systems of the El Garia Formation (Metlaoui Group, Lower Eocene), offshore Tunisia. In: MacGregor, D.S., Moody, R.T.J., Clark-Lowes, D.D. (Eds.), Petroleum Geology of North Africa. Geological Society Spec. Publ. No 132, pp. 355–374.
Lutze, G.F., 1964. Statistical investigations on the variability of *Bolivina argentea* Cushman. Cushman Found. Foraminiferal Res. Contribut. 15, 105–116.
Maaté, A., Martín-Algarra, A., Martín-Martín, M., Serra-Kiel, J., 2000. Nouvelles données sur le Paléocène-Eocène des zones internes bético-rifaines. Geobios 33 (4), 409–418.
Martín-Algarra, A., 1987. Evolución geológica Alpina del contacto entre las Zonas Internas y las Zonas Externas de la Cordillera Bética. Unplublished PhD Thesis. Univ. Granada, p. 1171.
Martín-Algarra, A., Alonso-Chaves, F., Andreo, B., Balanyá, J.C., Estévez, A., González-Lodeiro, F., Jabaloy, A., López-Garrido, A.C., Martín-Martín, M., O'Dogherty, L., Orozco, M., Rodríguez-Cañero, R., Ruiz-Cruz, M.D., Sánchez-Navas, A., Sanz de Galdeano, C., 2004. Complejo Maláguide. In: Vera, J.A. (Ed.), Geología de España. SGE-IGME, Madrid, pp. 401–409.
Martín-Martín, M., 1996. El Terciario del Dominio Maláguide en Sierra Espuña (Cordillera Bética oriental, SE de España): estratigrafía y evolución paleogeográfica. PhD Thesis. Univ. Granada, p. 297.
Martín-Martín, M., Martín-Algarra, A., Serra-Kiel, J., 1997a. El Terciario del Dominio Maláguide en Sierra Espuña (Prov. De Murcia, SE de España). Rev. Soc. Geol. Esp. 10 (3–4), 265–280.
Martín-Martín, M., El Mamoune, B., Martín-Algarra, A., Martín-Pérez, J.A., Serra-Kiel, J., 1997b. Timing of deformation in the Malaguide of the Sierra Espuña (Southeastern Spain). Geodynamic evolution f the Internal Betic Zone. Geol. Mijnb. 75 (4), 309–316.
Martín-Martín, M., Serra-Kiel, J., El Mamoune, B., Martín-Algarra, A., Serrano, F., 1998. The Paleocene of the Eastern Malaguides (Betic Cordillera, Spain): Stratigraphy and Paleogeography. C. R. Geosci. 326, 35–41.
Martín-Martín, M., Rey, J., Alcalá-García, F.J., Tosquella, J., Deramond, J., Lara-Corona, E., Duranthon, F., Antoine, P.O., 2001. Tectonic controls of the deposits of a foreland basin: an example from the Eocene Corbières-Minervois basin, France. Basin Res. 13, 419–433.
Martín-Martín, M., Martín-Rojas, I., Caracuel, J., Estévez-Rubio, A., Martín-Algarra, A., Sandoval, J., 2006. Tectonic framework and extensional pattern of the Malaguide complex from Sierra Espuña (internal betic zone) during jurassic-cretaceous: implications for the westernmost Tethys geodynamic evolution. Int. J. Earth Sci. 95, 815–826.
Martín-Martín, M., Guerrera, F., Tramontana, M., 2020a. Geodynamic implications of the latest Chattian-Langhian central-western peri-Mediterranean volcano-sedimentary event: a review. J. Geol. 128.
Martín-Martín, M., Guerrera, F., Miclaus, C., Tramontana, M., 2020b. Similar Oligo-Miocene tectono-sedimentary evolution of the Paratethyan branches represented by the Moldavidian Basin and Maghrebian Flysch Basin. Sediment. Geol. 396, 105548.
Martín-Martín, M., Guerrera, F., Tosquella, J., Tramontana, M., 2020c. Paleocene-Lower Eocene carbonate platforms of westernmost Tethys. Sediment. Geol. 404, 105674.
Martín-Martín, M., Guerrera, F., Tosquella, J., Tramontana, M., 2021. Middle Eocene carbonate platforms of the westernmost Tethys. Sediment. Geol. 415, 105861.
Mateu-Vicens, G., Khokhlova, A., Sebastián-Pastor, T., 2014. Epiphytic foraminiferal indices as bioindicators in mediterranean seagrass. J. Foraminifer. Res. 44 (3), 325–339.
Maticec, D., Vlahovic, I., Velic, I., Tisljar, J., 1996. Eocene limestones overlying lower cretaceous deposits of Western lstria (Croatia): did some parts of present lstriam form land during the cretaceous? Geol. Croatica 49 (1), 117–127.
Matteucci, R., 1996. Autecologic remarks on recent and fossil Haddonia (Textulariina, Foraminifera). In: Cherchi, A. (Ed.), Autecology of Selected Fossil Organisms: Achievements and Problems. Bollettino della Società Paleontologica Italiana, Special Volume, 3, pp. 113–122.
Michel, J., Borgomano, J., Reijmer, J.G., 2018. Heterozoan carbonates: when, where and why? A synthesis on parameters controlling carbonate production and occurrences. Earth Sci. Rev. 182, 50–67.
Molina, E., Cosovic, V., Gonzalvo, C., von Salis, K., 2000. Integrated biostratigraphy across the Ypresian/Lutetian boundary at Agost. Spain. Revue de Micropaléontol. 43 (3), 381–391.
Morsilli, M., Hairabian, A., Borgomano, J., Nardon, S., Adams, E., Bracco Gartner, G., 2017. The apulia carbonate platform-gargano promontory, Italy (Upper Jurassic–Eocene). AAPG Bull. 101 (4), 523–531.
Müller, R.D., Zahirovic, S., Williams, S.E., Cannon, J., Seton, M., Bower, D.J., Tetley, M. G., Heine, C., Le Breton, E., Liu, S., Russell, S.H.J., Yang, T., Leonard, J., Gurnis, M., 2019. A global plate model including lithospheric deformation along major rifts and orogens since the Triassic. Tectonics 38.
Murray, J.W., 2006. Ecology and Applications of Benthic Foraminifera. Cambridge University Press, p. 426.
Mutti, M., Hallock, P., 2003. Carbonate systems along nutrient and temperature gradients: some sedimentological and geochemical constraints. Int. J. Earth Sci. 92 (4), 465–475.
Nebelsick, J.H., Bassi, D., 2000. Diversity, growth forms and taphonomy: key factors controlling the fabric of coralline algae dominated shelf carbonates. In: Insalaco, E., Skelton, P.W., Palmer, T.J. (Eds.), Carbonate Platform Systems: Components and Interactions. Geological Society London, 178. Special Publication, pp. 89–107.
Nebelsick, J.H., Rasser, M.W., Bassi, D., 2005. Facies dynamics in Eocene to Oligocene circumalpine carbonates. Facies 51, 197–216.
Nebelsick, J.H., Bassi, D., Lempp, J., 2013. Tracking paleoenvironmental changes in coralline algal-dominated carbonates of the Lower Oligocene Calcareniti di Castelgomberto formation (Monti Berici, Italy). Facies 59 (1), 133–148.
Obiosio, E.O., 2013. Biostratigraphy and Paleoenvironment of *Bolivina* Fauna from the Niger Delta. Nigeria. Earth Sci. Res. 2 (2), 80–92.
Ortiz, S., Thomas, E., 2006. Lower-middle Eocene benthic foraminifera from the Fortuna Section (Betic Cordillera, southeastern Spain). Micropaleontology 52 (2), 97–150.
Özcan, E., Less, G., Okay, A.I., Baldi-Beke, M., Kollanyi, K., Yilmaz, I.O., 2010. Stratigraphy and larger foraminifera of the eocene shallow-marine and olistostromal units of the Southern Part of the Thrace Basin, NW Turkey. Turk. J. Earth Sci. 19, 27–77.
Perri, F., Critelli, S., Martín-Martín, M., Montone, S., Amendola, U., 2017. Unravelling hinterland and offshore palaeogeography from pre-to-syn-orogenic clastic sequences of the Betic Cordillera (Sierra Espuña), Spain. Palaeogeogr. Palaeoclimatol. Palaeoecol. 468, 52–69.
Perry, C.T., Beavington-Penney, S.J., 2005. Epiphytic calcium carbonate production and facies development within sub-tropical seagrass beds, Inhaca Island, Mozambique. Sediment. Geol. 174, 161–176.
Poblet, J., Muñoz, J.A., Travé, A., Serra-Kiel, J., 1998. Quantifying the kinematycs of detachment folds using three-dimensional geometry: application to the Mediano anticline (Pyrenees, Spain). Geol. Soc. Am. Bull. 110 (1), 11–125.
Pomar, L., 2001. Types of carbonate platforms: a genetic approach. Basin Res. 13, 313–334.
Pomar, L., Baceta, J.I., Hallock, P., Mateu-Vicens, G., Basso, D., 2017. Reef building and carbonate production modes in the west-central Tethys during the Cenozoic. Mar. Pet. Geol. 83, 261–304.
Racey, A., 2001. A review of eocene nummulite accumulations: structure, formation and reservoir potential. J. Pet. Geol. 24 (1), 79–100.
Rasser, M.W., 2000. Coralline red algal limestones of the Late Eocene Alpine foreland basin in Upper Austria: component analysis, facies and paleoecology. Facies 42, 59–92.
Rasser, M.W., Piller, W.E., 2004. Crustose algal frameworks from the Eocene Alpine Foreland. Palaeogeogr. Palaeoclimatol. Palaeoecol. 206, 21–39.
Reich, S., Di Martino, E., Todd, J.A., Wesselingh, F.P., Renema, W., 2015. Indirect paleo-seagrass indicators (IPSIs): a review. Earth Sci. Rev. 143, 161–186.
Reuter, M., Piller, W.E., Harzhauser, M., Kroh, A., Rögl, F., Coric, S., 2011. The Quilon Limestone, Kerala Basin, India: an archive for Miocene Indo-Pacific seagrass beds. Lethaia 44, 76–86.
Rodríguez-Pintó, A., Pueyo, E.L., Serra-Kiel, J., Samsó, J.M., Barnolas, A., Pocoví, A., 2012. Lutetian magnetostratigraphic calibration of larger foraminifera zonation (SBZ) in the southern Pyrenees: the Isuela section. Palaeogeogr. Palaeoclimatol. Palaeoecol. 333–334, 107–120.
Romero, J., Caus, E., Rosell, J., 2002. A model for the palaeoenvironmental distribution of larger foraminifera based on late Middle Eocene deposits on the margin of the South Pyrenean basin (NE Spain). Palaeogeogr. Palaeoclimatol. Palaeoecol. 179, 43–56.
Roozpeykar, A., Moghaddam, I.M., 2016. Sequence biostratigraphy and paleoenvironmental reconstruction of the Oligocene-early Miocene deposits of the Zagros Basin (Dehdasht area, South West Iran). Arab. J. Geosci. 9, 77.
Roozpeykar, A., Maghfouri-Moghaddam, I.M., Yazdi, M., Yousefi-Yegane, B., 2019. Facies and paleoenvironmental reconstruction of Early–Middle Miocene deposits in the north-west of the Zagros Basin. Iran. Geol. Carpathica 70 (1), 75–87.
Sarkar, S., 2019. Alveolina-dominated assemblages in the early Eocene carbonates of Jaintia Hills, NE India: biostratigraphic and palaeoenvironmental implications. C. R. Palevol. 18, 949–966.
Scheibner, C., Speijer, R.P., 2008. Late Paleocene-Early Eocene Tethyan carbonate platform evolution - A response to long- and short-term paleoclimatic change. Earth Sci. Rev. 90, 71–102.
Serra-Kiel, J., Hottinger, L., Caus, E., Drobne, K., Ferràndez, C., Jauhri, A.K., Less, G., Pavlovec, R., Pignatti, J., Samsó, J.M., Schaub, H., Sirel, E., Strougo, A., Tambareau, Y., Tosquella, J., Zakrevskaya, E., 1998. Larger foraminiferal biostratigraphy of the Thetian Paleocene and Eocene. Bull. Soc. Géol. France 169 (2), 281–299.
Serra-Kiel, J., Travé, A., Mató, E., Saula, E., Ferràndez-Cañadell, C., Busquets, P., Tosquella, J., Vergés, J., 2003a. Marine and transitional Middle/Upper Eocene units of the southeastern Pyrenean foreland basin (NE Spain). Geol. Acta 1 (2), 177–200.
Serra-Kiel, J., Mató, E., Saula, E., Travé, A., Ferràndez-Cañadell, C., Busquets, P., Samsó, J.M., Tosquella, J., Barnolas, A., Álvarez-Pérez, G., Franquès, J., Romero, J., 2003b. An inventory of the marine and transitional Middle/Upper Eocene deposits of the Southeastern Pyrenean Foreland Basin (NE Spain). Geol. Acta 1 (2), 201–229.

Serra-Kiel, J., Gallardo-Garcia, A., Razin, Ph., Robinet, J., Roger, J., Grelaud, C., Leroy, S., Robin, C., 2016. Middle Eocene-Early Miocene larger foraminifera from Dhofar (Oman) and Socotra Island (Yemen). Arab. J. Geosci. 9 (5), 1–95.
Serrano, F., 1997. La Cordillera Bética en la provincia de Málaga. In: Rebollo, M., Serrano, F., Nieto, J.M., Cabezudo, B. (Eds.), Itinerarios por espacios naturales de la Provincia de Málaga. Una aproximación al conocimiento de su geología y su botánica, 75–112. Serv. Public. Univ. de Málaga. ISBN: 84–7496–664-7.
Serrano, F., Guerra-Merchán, A., 2004. Geología de la provincia de Málaga, 294 pp. CEDMA (Servicio de Publicaciones de la Diputación de Málaga). ISBN: 84–7785–654-0.
Serrano, F., Sanz de Galdeano, C., Delgado, F., López-Garrido, A.C., Martín-Algarra, A., 1995. The Mesozoic-Cenozoic of the Malaguide Complex in the Málaga area: a Paleogene olistostrome-type chaotic complex (Betic Cordillera, Spain). Geol. Mijnb. 74, 105–116.
Silva-Casal, R., Aurell, M., Payros, A., Pueyo, E.L., Serra-Kiel, J., 2019. Carbonate ramp drowning caused by flexural subsidence: The South Pyrenean middle Eocene foreland basin. Sediment. Geol. 393–394, 105538.
Smith, C., 2015. Distribution of encrusting foraminifera at Cat Island, Bahamas: Implications for foraminiferal assemblages in the geologic record. Graduation Thesis. Auburn University, Alabama.
Solé de Porta, N., Jaramillo, C.A., Algarra-Martin, A., 2007. Pantropical palynomorphs in the Eocene of the Malaguides (Betic Range, Southern Spain). Rev. Esp. Micropaleontol. 39, 189–204.
Spanicek, J., Cosovic, V., Mrinjek, E., Vlahovic, I., 2017. Early Eocene evolution of carbonate depositional environments recorded in the Cikola Canyon (North Dalmatian Foreland Basin, Croatia). Geol. Croat. 70, 11–25.
Taberner, C., Bosence, D.W.J., 1985. Ecological succession from corals to coralline algae in Eocene patch reefs, Northern Spain. In: Toomey, D.F., Nitecki, M.H. (Eds.), Palaeoalgology, Contemporary Research and Applications: 226–236. Springer-Verlag, Berlin.
Tawfik, M., El-Sorogy, A., Moussa, M., 2016. Metre-scale cyclicity in Middle Eocene platform carbonates in northern Egypt: implications for facies development and sequence stratigraphy. J. Afr. Earth Sci. 119, 238–255.
Tomás, S., Frijia, G., Bömelburg, E., Zamagni, J., Perrin, C., Mutti, M., 2016. Evidence for seagrass meadows and their response to paleoenvironmental changes in the early Eocene (Jafnayn Formation, Wadi Bani Khalid, N Oman). Sediment. Geol. 341, 189–202.
Tomassetti, L., Benedetti, A., Brandano, M., 2016. Middle Eocene seagrass facies from Apennine carbonate platforms (Italy). Sediment. Geol. 335, 136–149.
Tosquella, J., Serra-Kiel, J., 1998. Los nummulítidos (Nummulites y Assilina) del Paleoceno Superior-Eoceno Inferior de la Cuenca Pirenaica: Sistemática. Acta Geol. Hisp. 31 (1996), 37–159.
Vescogni, A., Bosellini, F.R., Papazzoni, C.A., Giusberti, L., Roghi, G., Fornaciari, E., Dominici, S., Zorzin, R., 2016. Coralgal buildups associated with the Bolca Fossil-Lagerstätten: new evidence from the Ypresian of Monte Postale (NE Italy). Facies 62, 1–21.
Vlahovic, I., Tisljar, J., Velic, I., Maticec, D., 2005. Evolution of the Adriatic Carbonate Platform: palaeogeography, main events and depositional dynamics. Palaeogeogr. Palaeoclimatol. Palaeoecol. 220, 333–360.
Voermans, F.M., Geel, T., Baena-Pérez, J., 1978. Hoja 1:50.000 de Vélez Rubio (No 974). Plan MAGNA. IGME, Madrid.
Westphal, H., Halfar, J., Freiwald, A., 2010. Heterozoan carbonates in subtropical to tropical settings in the present and past. Int. J. Earth Sci. (Geologische Rundschau) 99 (Suppl. 1), S153–S169.
Whidden, K., Jones, R.W., 2012. Correlation of early paleogene global diversity patterns of large benthic foraminifera with Paleocene and Eocene climatic events. Palaios 27 (3), 235–251.
White, S., 2002. Encrusting foraminifera from Lee Stocking Island, Bahamas: taphonomy, shelf-to-slope distribution, and behavior. Graduation Thesis. The University of Rochester, Athens, Georgia.
Woelkerling, W.J., Irvine, L.M., Harvey, A.S., 1993. Growth-forms in non-geniculate coralline red algae (Corallinales, Rhodophyta). Aust. Syst. Bot. 6, 277–293.
Wood, R., 1993. Nutrients, predation and the history of reef-building. Palaios 8, 526–543.
Wray, J.L., 1977. Calcareous Algae. Elsevier Publishers, Amsterdam, p. 190.
Wright, V.P., Burgess, P.M., 2005. The carbonate factory continuum, facies mosaics and microfacies: an appraisal of some of the key concepts underpinning carbonate sedimentology. Facies 51, 17–23.
Zachos, J.C., Quinn, T.M., Salami, K.A., 1996. High-resolution (10^4 years) deep-sea foraminiferal stable isotope records of the Eocene-Oligocene climate transition. Paleoceanography 11 (3), 251–266.
Zachos, J.C., Pagani, M., Sloan, L.C., Thomas, E., Billups, K., 2001. Trends, rhythms, and aberrations in global climate 65Ma to present. Science 292, 686–693.